This document was prepared for the ETI by third parties under contract to the ETI. The ETI is making these documents and data available to the public to inform the debate on low carbon energy innovation and deployment.

Programme Area: Marine

Project: PerAWAT

Title: Representation of Wave Energy Converters in Spectral Wave Models

Abstract:

This deliverable is the first within the Wave sub-project. It describes the representation of wave energy converters in a third generation spectral wave model and begins by providing some background about the current state-of-the art for wave energy converter array representation. This is followed by the development of a general methodology for representing wave energy converters in a spectral-domain model, where the term spectral-domain model here refers to a numerical representation of the wave energy field which has been decomposed into frequency components. Emphasis is placed on the ability of a spectral domain model to capture the nonlinear characteristics of a wave energy converter. Initial cross validation is provided by comparison of the derived spectral-domain model with a time-domain model in two separate examples of nonlinear wave energy converter characteristics (wave force decoupling, and quadratic drag). Additional cross-validation of the method is demonstrated though comparison with physical wave tank experiments carried out at Queen's University Belfast. The deliverable subsequently focuses on the specific type of spectral-domain model that will be implemented in WG1 WG2, the spectral wave model, in which the wave energy converters will be represented.

Context:

The Performance Assessment of Wave and Tidal Array Systems (PerAWaT) project, launched in October 2009 with £8m of ETI investment. The project delivered validated, commercial software tools capable of significantly reducing the levels of uncertainty associated with predicting the energy yield of major wave and tidal stream energy arrays. It also produced information that will help reduce commercial risk of future large scale wave and tidal array developments.

Representation of wave energy converters in spectral wave models

WG1 WP2 D1

DOCUMENT CONTROL SHEET

Client	Energy Technology Institute
Contact	Geraldine Newton-Cross
Project Title	PerAWaT
Document N^{o}	QUB-101124
Classification	Not to be disclosed except in line with the terms of the Technology Contract
Date	30th March 2011

REV.	Issue date	Purpose of issues	Prepared by	Checked by
0.01	7/12/2010	Draft for review	KS	MF
0.02	12/12/2010	Changes for comments	KS	MF
0.03	14/12/2010	Draft for comments from GH	KS	MF
0.04	15/12/2010	Executive summary and references added	KS	MF
1.00	21/12/2010	Preliminary release to GH	KS	MF
2.00	29/12/2010	Release to GH/ETI	MF	
3.00	17/02/2011	Revised in response to ETI comments	KS	MF
4.00	30/03/2011	Minor revisions	MF	KS

Approved for release by: Matt Folley

Contents

Executive Summary

This document describes the representation of wave energy converters in a third generation spectral wave model and begins by providing some background about the current state-of-the art for wave energy converter array representation. This is followed by the development of a general methodology for representing wave energy converters in a spectral-domain model, where the term "spectral-domain model" here refers to a numerical representation of the wave energy field which has been decomposed into frequency components. Emphasis is placed on the ability of a spectral-domain model to capture the nonlinear characteristics of a wave energy converter. Initial cross-validation is provided by comparison of the derived spectral-domain model with a time-domain model in two separate examples of nonlinear wave energy converter characteristics (wave force decoupling, and quadratic drag). Additional cross-validation of the method is demonstrated though comparison with physical wave tank experiments carried out at Queen's University Belfast.

The deliverable subsequently focuses on the specific type of spectral-domain model that will be implemented in WG1 WG2, the spectral wave model, in which the wave energy converters will be represented. Background information is provided about the development of spectral wave models. Then, the wave action density equation, which is the main equation solved by spectral wave models, is described in detail. The relationship of spectral wave models to other types of wave models, including time-domain models such as mild slope equation and Boussinesq models, is discussed. In particular, a major difference between spectral wave models and other wave model types is the phase averaging assumption, which says that the phases of individual waves in a wave field can be represented with a random distribution. Previous numerical studies have suggested that spectral wave models may be incapable of an accurate representation of wave energy converter because the phase averaging assumption doesn't allow for capture of phase-dependent array interaction processes. However, it is shown that these studies are potentially misleading because they represent idealized situations. A simple numerical model of a two wave energy converter array is used to demonstrate that when a more realistic configuration is used (i.e. one that accounts for uncertainties associated with the wave field and the device characteristics) array interaction factors are reduced; this provides justification for representing wave energy converters using a phase averaging model.

Next, the formulation of a wave energy converter in a spectral wave model is addressed. The few published studies which have implemented an array of wave energy converters in a spectral wave model have used a supra-grid representation, where the effect of the wave farm is modelled as a

single entity. The strengths and weaknesses of this approach are discussed. A new, sub-grid, representation is described and justified for use in the WG1 WP2 work plan. This sub-grid method will allow wave energy converters to be represented as source terms in the wave action equation. The advantage of this method is the ability to easily represent the frequency, directional, and even wave state dependence of the wave energy converter effect on wave action.

Finally, the derivation of the specific expression to be used to incorporate a wave energy converter in a spectral wave model is presented. The source strength of wave energy converter in the wave action equation is broken down into three major physical mechanisms, including reflection of incident wave energy due to the presence of the wave energy converter, radiation of energy due to the motion of the wave energy converter, and extraction of energy both by the wave energy converter and by dissipation of energy due to turbulence around the device. The flexibility of the representation of WECs is discussed and it is concluded that any WEC, including all the fundamental device concepts, may be represented in a spectral wave model. A method for solving the source terms is described, and an example for a point absorber wave energy converter is presented to provide an indication of the type of information required to define a WEC.

1 Introduction

1.1 Scope of document

The objective of PerAWaT Work Group 1 Work Package 2 is to develop an add-on to a spectral wave model software tool that enables wave energy converters (WECs) to be represented robustly and accurately. This will allow accurate and computationally efficient estimates of the productivity of wave farms. The purpose of this document is to describe the WEC representation that will be used along with supporting evidence from preliminary cross-validation exercises. Following the Introduction, Section 2 presents a general derivation for the representation of average power capture of a WEC in a spectral-domain model. Here, a spectral-domain model is defined as any numerical representation of the wave energy field which has been decomposed into frequency components and allows the representation of non-linear components. The spectral-domain power equation for a WEC is then implemented and compared with a time-domain model of a heaving buoy and with wave tank data of an oscillating water column (OWC) model. In this configuration the OWC is acting as a point absorber with fundamentally the same hydrodynamics; it is thus an example of one of the key fundamental device concepts. Section 3 provides an overview of spectral wave models (a special type of spectral-domain model which solves the wave action density conservation equation), and provides a justification of the use of a phase-averaged model for representing large numbers of wave energy devices. Section 4 compares two options for physical representation of a wave energy converter in model grid space, and describes which option was chosen for implementation in the PerAWaT project. Finally, Section 5 derives the expression for representing a wave energy converter in a third generation spectral wave model, and provides an example representation for a floating heaving buoy-type (point absorber) wave energy converter.

1.2 Modelling of wave energy converter arrays

It was recognised early in the development of numerical models for wave energy converters that array interactions may be important to their performance (Falnes 1980, Thomas and Evans 1981). As a consequence a frequency-domain model, based on linear potential flow theory (See for example, Falnes 2002), of the interaction between wave energy converters was developed and the maximum array interaction factor calculated for different array configurations (Thomas and Evans 1981, Fitzgerald and Thomas, 2007), including different methods for solving the potential flow problem (Simon, 1982; McIver, 1994; Mavrakos and McIver, 1997). The array interaction factor is the change in power capture of a device in an array relative to the power capture of the device in isolation. Based on the assumptions of linear hydrodynamics, together with an assumption of ideal

control it was shown that array interactions can significantly increase the power capture of an array (Fitzgerald and Thomas, 2007). Indeed, it is shown that power capture can theoretically more than double for particular array configurations. The array interaction factor was found to peak at 2.77 for a group of 5 heaving buoy with an irregular configuration covering an area of 6x3 wavelengths (in a linear hydrodynamic model the optimum array configuration is a function of the wavelength).

Unfortunately there has been very little physical modelling of WEC arrays and the little that has been done has not been reported in peer-reviewed publications. It is likely that this is in part due to the difficulty in controlling a wave-tank sufficiently for the array interactions of small WEC arrays to be clear above the effect of wave-tank aberrations. For example, even with effective beaches, which have a reflection coefficient less than 0.1, the power capture of an isolated device can vary by more than 50% (the difference in power captures at partial nodes and anti-nodes) (Folley 2010). It is also likely to be due to the requirement that some WECs in the array must feed power back into the waves (i.e. be driven) to obtain the maximum array interaction factors, which is difficult to achieve with a real device (but not a restriction for a numerical model).

More recently numerical modelling of WEC arrays has looked at the array interaction factors for WECs will sub-optimal control, which is more similar to that which may be achieved with a realistic device (Justino and Clement, 2003; Thomas et al., 2008; Folley and Whittaker 2009). It is shown that without ideal control the array interaction factors are much smaller. It has also been shown for each area of constructive interference, which creates a positive array interaction, there is an area of destructive interference, which creates a negative array interaction (Fitzgerald and Thomas, 2007). Finally, it has been shown that the bandwidth of array interaction factors is extremely narrow and that for a fixed layout the maximum average array interaction factor at a typical North Atlantic site for a wave farm is about 1.1; sub-optimal control and motion constraints are likely to reduce this further (Folley and Whittaker 2009). This does not mean that array interactions are not important, but that the earlier work is perhaps of limited value due to the unrealistic assumptions that were made regarding the incident waves and WEC control. Indeed, it has been shown that control can influence the power capture of a wave farm and this can be optimised to maximise the wave farm productivity (Cruz et al., 2009).

Time-domain models have also been developed for array interactions, which have also been based on linear potential flow theory (Babarit et al., 2009). These models have been demonstrated for a pair of WECs. By using a time-domain simulation it is possible to include the effect of non-linear components on the power capture, with the assumption that the hydrodynamic coefficients defined

by the linear potential flow theory remain unchanged. Because optimal control of a WEC is acausal (the incident wave into the future must be known to define the optimal control) the time-domain model was sub-optimal. Not surprisingly the array interactions factors were found to be smaller than the maximums obtained from the frequency-domain models, with maxima less than 1.4 (with averages of about 1.0 – i.e. minimal change in power capture due to array interactions). However, because the array modelled contained only 2 WECs it is not surprising that the array interactions were relatively small.

Wave farms have also been modelled using wave propagation models including a Boussinesq model (Venugopal and Smith, 2007) and a third generation spectral wave model (Millar, 2006). However, in both cases the attributes of the wave farm have been assigned, with the implicit assumption that array interactions have been calculated elsewhere and used to produce the wave farm model. Mild-slope wave propagation models have also been used to model WEC array interactions, although this has only been implemented for the WaveDragon, which is a floating over-topping type WEC and large relative to the typical wavelength at the deployment location (Beels et al. 2009). No physical cross-validation of these models has been performed.

Most recently it has been suggested that wave energy converters could be represented in third generation spectral wave models as additional wave action density source terms, which extract and re-distribute energy in the spatial, frequency and directional dimensions (Folley and Whittaker, 2010). In this case it is proposed that array interactions are achieved using the wave propagation model of the spectral wave model. However, the representation of WECs in spectral wave models has only been suggested and the actual form that the WEC source term may take and the inclusion of them in a spectral wave model has not been considered in detail. It is the objective of this work package of the PerAWaT project to progress the modelling of WEC arrays in this way.

1.3 Relationship to other deliverables

This deliverable is closely linked to WG1 WP2 D2 (*Implementation of wave energy converters in spectral wave models*). WG1 WP2 D2 addresses some of the more practical issues associated with the project, including which software tools will be used, how the code development will be structured, and the description of testing which will be used to verify the functionality and stability of the code.

1.4 WG1 WP2 D1 acceptance criteria

The acceptance criteria for this deliverable and WG1 WP2 D2 were defined together, and are as follows:

1. *Report contains full description of theory and underlying assumptions in model to enable a full review by a third party.*
2. *Report contains sufficient detail for implementation of model in software code to be understood by a third party together with specification of test cases.*
3. *Model covers full range of WEC FDCs as agreed in WG0*

The first and third criteria are applicable to this deliverable. In order to satisfy the first criterion with this deliverable, a theory for spectral-domain modelling of wave energy converters is developed and cross-validated in section 2 of this document. Spectral wave models are described in detail in section 3, including their inherent assumptions. Finally, the theory which will support the representation of wave energy converters in a spectral wave model is discussed in Section 4 and developed in Section 5. The representation that is developed in Section 5 is sufficiently general to be applicable to any wave energy converter, thus satisfying the third of the acceptance criteria.

2 Spectral domain modelling of wave energy converters

2.1 Overview

The first numerical representations of wave energy converters to be developed were frequency-domain models which are based on linear hydrodynamics (Falnes and Budal, 1987; Evans, 1980; Falnes, 1980; Mei and Newman, 1980; Evans, 1981, 1985). In linear hydrodynamics, a system output is proportional to the input, and it is assumed that the components of the wave field can simply be summed to give the total wave field. In a frequency-domain model, the sea state is decomposed into a set of sinusoidal frequency components. Wave energy converter hydrodynamics are calculated for each frequency independently and results for each frequency can be summed over the spectrum to give the full wave energy converter response. However, this method does not account for non-linear processes, making the models inaccurate. The current alternative to frequency-domain models of wave energy converters is the time-domain model, which has the advantage of allowing non-linear terms to be incorporated into the equations of motion easily. Time-domain models can be formulated as the Fourier transform of a frequency domain equation, which results in a differential integral equation known as the Cummins equation (see for example, Newman, 1977). Because a Cummins equation time-domain model can be difficult to solve, a Laplace transfer function formulation (or equivalent) of the time-domain model could be used instead (McCabe et al, 2007). A Laplace transfer function formulation effectively adds degrees of freedom to the wave energy converter model to represent the motion of the sea. The Laplace

transfer function formulation is generally less computationally intense than a Cummins equation model. However, in general time-domain models are much more computationally intensive than frequency-domain models, and therefore are not a viable solution for modelling arrays of wave energy converters and where several scenarios may need to be investigated.

This section describes an extension to frequency-domain modelling of wave energy converters which allows nonlinear terms to be approximated, which is here called spectral-domain modelling. In general a spectral-domain model uses the wave spectrum as the wave input and typically calculates the spectral variance density of the WEC response together with aggregated parameters such as the power generated. This approach has the benefit of a significantly quicker computation time than time-domain modelling whilst achieving higher accuracy than frequency-domain models by incorporating nonlinear terms. Spectral-domain modelling uses the assumption that the phases of individual waves are randomly distributed, and therefore is unable to explicitly represent phase-dependent processes like diffraction and refraction. The assumption of random phase is implicit in any representation of a sea-state that uses a spectrum; although this assumption is not always fully recognised. Comparison with both a time-domain model and wave tank model data demonstrates the ability of the derived spectral-domain model to represent the power capture of wave energy converters. This work serves as preliminary cross-validation that wave energy converters can be represented in spectral-domain models. The actual expression for incorporation of a wave energy converter into a third generation spectral wave model is described in Section 5, and the cross-validation of this specific approach will occur throughout the PerAWaT program with comparison to both wave tank data (WG2 WP1/2), and linear and nonlinear hydrodynamic modelling (WG1 WP1).

2.2 Modelling wave energy converters using spectral-domain models

A spectral-domain model can be any numerical representation which decomposes the wave field into frequency components and has some way of accounting for nonlinear interactions. This can in general be any function, which may have been derived analytically or heuristically. In the examples presented here, a spectral-domain model for the power of a wave energy converter with a quasi-linear approximation of nonlinear terms is derived analytically. The approximation of the nonlinear terms is considered quasi-linear because the model is linear except for the model coefficients, which are functions of the total model response. Solution of this model requires iteration until the model coefficients produce a response that is effectively the same as that used to define them. A quasi-linear spectral approximation of nonlinear wave processes such as dissipation due to whitecapping was developed years ago for implementation in third generation spectral wave models (Hasselman et. al, 1974). It is straightforward to extend this approximation to the

representation of a wave energy converter. In particular, we wish to derive an expression for the average power of a wave energy converter, which is equal to the expected value (denoted by $\langle \dots \rangle$) of the product of the body force **F** and the velocity of the body on which the force acts, **U,** as given by $\boldsymbol{P} = \langle \boldsymbol{FU} \rangle$. Here, the expected value represents a weighted time average. The body velocity can be represented as the sum of a set of sinusoidal velocity components: $\boldsymbol{U} = \sum_{\boldsymbol{j}} \boldsymbol{u_j} = \sum_j \omega_j a_j \cos(\omega_j t + \varphi_j)$. The body force, ***F***, is the function of both the body velocity ***U***, and any external parameters (represented here by β): $\boldsymbol{F} = \boldsymbol{F}(\boldsymbol{U}, \boldsymbol{\beta})$. The external parameter $\boldsymbol{\beta}$ represents any other variable which the force is dependent on; one example of an external parameter is the wave force. The external parameters can be broken down into frequency components as $\boldsymbol{\beta} = \sum_{\boldsymbol{j}} \boldsymbol{\beta_j}$, where the $\boldsymbol{\beta_j}$ vary in space and time and are not necessarily sinusoidal. Because the dependent variables $\boldsymbol{U}$ and $\boldsymbol{\beta}$ are decomposed into many frequency components, each individual component is considered infinitesimal. The expression for the average power of a wave energy converter becomes

$$\boldsymbol{P} = \sum_{\boldsymbol{j}} \langle \boldsymbol{F}\left(\boldsymbol{u_1}, \boldsymbol{u_2}, \dots, \boldsymbol{u_j}, \dots, \boldsymbol{u_n}, \boldsymbol{\beta_1}, \dots, \boldsymbol{\beta_n}\right) \boldsymbol{u_j} \rangle = \sum_{\boldsymbol{j}} \langle \boldsymbol{F}(\boldsymbol{Z}) \boldsymbol{u_j} \rangle, \qquad (2.1)$$

$$\text{where } \boldsymbol{Z} \equiv \left(\boldsymbol{u_1}, \boldsymbol{u_2}, \dots, \boldsymbol{u_j}, \dots, \boldsymbol{u_n}; \boldsymbol{\beta_1}, \boldsymbol{\beta_2}, \dots, \boldsymbol{\beta_j}, \dots, \boldsymbol{\beta_n}\right). \qquad (2.2)$$

The dependent variable field **Z** can be decomposed as follows: $\boldsymbol{Z} = \boldsymbol{Z_j'} + (\boldsymbol{u_j}, \boldsymbol{\beta_j})$**.** This gives $\boldsymbol{Z_j'} = (\boldsymbol{u_1}, \boldsymbol{u_2}, \dots, 0, \dots, \boldsymbol{u_n}; \boldsymbol{\beta_1}, \boldsymbol{\beta_2}, \dots, 0, \dots, \boldsymbol{\beta_n})$. In order to approximate the power in a quasi-linear way, a Taylor series expansion of the body force is performed around the variable $\boldsymbol{Z_j'}$. Keeping only the first order terms of the Taylor series results in the following approximation for the average power of a wave energy converter:

$$\boldsymbol{P} = \sum_{\boldsymbol{j}} \langle \left(\boldsymbol{F}\left(\boldsymbol{Z_j'}\right) + \frac{\boldsymbol{\partial F}}{\boldsymbol{\partial u_j}}\left(\boldsymbol{Z_j'}\right) \boldsymbol{u_j} + \frac{\boldsymbol{\partial F}}{\boldsymbol{\partial \beta_j}}(\boldsymbol{Z_j'}) \boldsymbol{\beta_j} \right) \boldsymbol{u_j} \rangle \qquad (2.3)$$

The body force $\boldsymbol{F}(\boldsymbol{Z_j'})$and the body velocity component $\boldsymbol{u_j}$ are uncorrelated, and the expected value of their product can be written as the product of their expected values, that is $\langle AB \rangle = \langle A \rangle \langle B \rangle$:

$$\boldsymbol{P} = \sum_{\boldsymbol{j}} \left[\langle \boldsymbol{F}(\boldsymbol{Z_j'}) \rangle \langle \boldsymbol{u_j} \rangle + \langle \frac{\boldsymbol{\partial F}}{\boldsymbol{\partial u_j}}\left(\boldsymbol{Z_j'}\right) \rangle \langle \boldsymbol{u_j^2} \rangle + \langle \frac{\boldsymbol{\partial F}}{\boldsymbol{\partial \beta_j}}(\boldsymbol{Z_j'}) \rangle \langle \boldsymbol{u_j \beta_j} \rangle \right] \qquad (2.4)$$

The first term on the right hand side of the above equation is zero because the expected value of the sinusoidal velocity components is zero. The resulting expression can be written in terms of two coefficients: $\boldsymbol{A_j} = \langle \frac{\boldsymbol{\partial F}}{\boldsymbol{\partial u_j}}(\boldsymbol{Z}) \rangle$ and $\boldsymbol{B}_j = \langle \frac{\boldsymbol{\partial F}}{\boldsymbol{\partial \beta_j}}(\boldsymbol{Z}) \rangle$, resulting in a final expression for the average power of a wave energy converter as follows:

$$\boldsymbol{P} = \sum_j \left[\boldsymbol{A_j} \langle \boldsymbol{u_j^2} \rangle + \boldsymbol{B_j} \langle \boldsymbol{u_j \beta_j} \rangle \right] \quad (2.5)$$

Note that the derivative terms are evaluated at $\boldsymbol{Z}$ instead of $\boldsymbol{Z_j'}$ because they only differ by an infinitesimal amount.

It will be noted that for any particular scenario the two coefficients, $\boldsymbol{A_j}, \boldsymbol{B_j}$, are constant and the model is quasi-linear (the coefficients depend on the response at all frequencies). This means that although to obtain the final solution the model requires an iterative process, but at each iteration only a linear system needs to be solved. Linear systems can generally be solved easily and very efficiently, making the spectral-domain model a highly attractive model. Final specification of the spectral-domain model requires that the exact form of the two coefficients, $\boldsymbol{A_j}, \boldsymbol{B_j}$, be determined.

2.3 Cross-validation of a spectral-domain model of a wave energy converter

2.3.1 Comparison of a spectral-domain model with a time-domain model

In order to provide cross-validation that the expression derived is appropriate when applied to wave energy converter modelling, a comparison of spectral-domain and time-domain models was carried out. In this case it is a cross-validation because it is determined whether the spectral-domain model is a valid model of a time-domain model, for irregular waves. Whether the time-domain model itself is a valid representation of a WEC is not investigated; however, the time-domain model used is typical for those used to represent the performance of WECs.

The device modelled is Oyster (Folley, 2010), which is a bottom-hinged, flap-type wave energy converter. Although this is not exactly one of the fundamental device concepts (FDCs) defined in WG0 D1, the Oyster representation used has a single degree of freedom and is very similar to a point absorber. The time-domain model of Oyster uses the Cummins Equation (see for example Newman, 1977, pg.310) and is implemented in Simulink, using a variable-step Dormand–Prince explicit Runge–Kutta formulation solver. The numerical model of Oyster contains the Cummins Equation for the hydrodynamic coefficients, $\mathrm{I}_\infty \dot{\boldsymbol{U}} + \int_0^{\mathrm{t}} \mathrm{G}(\tau) \boldsymbol{U}(\mathrm{t}-\tau)\mathrm{d}\tau$, together with the flap inertial force, $\mathrm{I}\dot{\boldsymbol{U}}$**,** the flap spring force, $\mathrm{k_p}\boldsymbol{A}$**,** a linear power-take-off (PTO) component, $\lambda \boldsymbol{U}$, and a non-linear (quadratic) drag component, $C_d \boldsymbol{U}|\boldsymbol{U}|$**,** and is shown in Equation (2.6) below.

$$\mathrm{T_w} = (\mathrm{I} + \mathrm{I}_\infty)\dot{\boldsymbol{U}} + \int_0^{\mathrm{t}} \mathrm{G}(\tau)\boldsymbol{U}(\mathrm{t}-\tau)\mathrm{d}\tau + \mathrm{k_p}\boldsymbol{A} + \lambda \boldsymbol{U} + C_d \boldsymbol{U}|\boldsymbol{U}| \quad (2.6)$$

Where the incident wave force, T_w, is produced by the summation of approximately 1000 individual frequency components from a Bretschneider spectrum using a random phase between frequency components.

The first model comparison uses the expression derived in the previous section to describe the nonlinear drag which is expressed as a quadratic damping term and represents the effects of turbulence on the flap device. Morrison's equation defines the drag force as: $\boldsymbol{F}_d = C_d\boldsymbol{U}|\boldsymbol{U}|$. Decomposing the velocity into sinusoidal components yields:

$$\boldsymbol{F}_d = C_d\big(u_1 + \cdots + u_j + \cdots + u_n\big)|u_1 + \cdots + u_j + \cdots + u_n| \tag{2.7}$$

Using the expression for the average power of a wave energy converter derived above while taking into account the fact that there are no external parameters for this test case (i.e. $\boldsymbol{B}_j$ is zero) gives:

$$\boldsymbol{P} = \sum_j\big[\boldsymbol{A}_j\langle\boldsymbol{u}_j^2\rangle\big] = \sum_j\frac{\partial \boldsymbol{F}_d}{\partial \boldsymbol{u}_j}\langle\boldsymbol{u}_j^2\rangle = \sum_j\langle\boldsymbol{2C_d}|\boldsymbol{u}|\rangle\,\langle\boldsymbol{u}_j^2\rangle \tag{2.8}$$

where the quasi-linear coefficient is expressed as:

$$\boldsymbol{A}_j = \langle\boldsymbol{2C_d}|\boldsymbol{u}|\rangle \tag{2.9}$$

This expression shows that the total average power dissipated due to quadratic damping can be accounted for by summing up the product of the expected value of the absolute velocity with the velocity components squared. This equation was iterated along with the equation of motion as a spectral-domain model as shown in Equation (2.10) below, and then compared to the time-domain model.

$$\mathbf{T_w}(\boldsymbol{\omega}) = \big[\big\{\boldsymbol{k_p} - (\boldsymbol{I} + \boldsymbol{I_a}(\boldsymbol{\omega}))\boldsymbol{\omega^2}\big\} + \boldsymbol{j}\{\mathbf{B}(\boldsymbol{\omega}) + \boldsymbol{\lambda} + \langle\boldsymbol{2C_d}|\boldsymbol{u}|\rangle\}\boldsymbol{\omega}\big]\boldsymbol{\Theta}(\boldsymbol{\omega}) \tag{2.10}$$

where $\boldsymbol{\omega}$ is the frequency of the wave component, $\mathbf{T_w}(\boldsymbol{\omega})$, $\boldsymbol{I_a}(\boldsymbol{\omega})$, $\mathbf{B}(\boldsymbol{\omega})$ are the frequency dependent wave torque, added mass and radiation damping coefficients respectively, $\boldsymbol{k_p}$ is the flap pitch stiffness coefficient, $\boldsymbol{\lambda}$ is the PTO damping coefficient, $\boldsymbol{C_d}$ is the drag coefficient, $|\boldsymbol{u}|$ is the expected value of the absolute velocity and $\boldsymbol{\Theta}(\boldsymbol{\omega})$ is the frequency-dependent amplitude of motion.

Examination of the Oyster power capture and power loss for both models demonstrates that the spectral-domain model produces a reasonable estimate of both quantities for a wide range of possible drag coefficients, including very large drag coefficients resulting in highly nonlinear system (Figures 1 and 2). Comparison of the velocity spectrum shows that the spectral-domain and time-domain models have the same basic shape, which means that the two models are producing similar

levels of power dissipation and power capture at each frequency (Figure 3). The ability of the spectral-domain model to capture both the correct power levels and spectral shapes (as defined in the time-domain model) suggests that spectral-domain modelling is indeed capable of representing the nonlinear aspects of a wave energy converter.

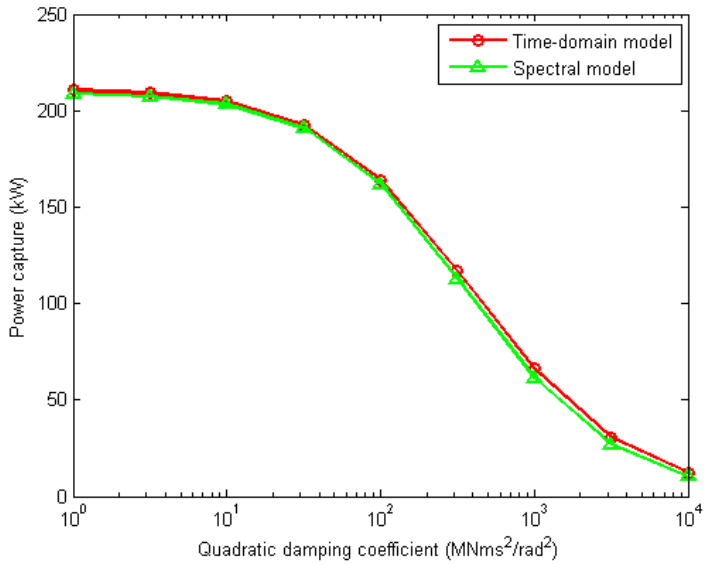

Figure 1: Comparison of estimated power capture for Oyster using time-domain and spectral models.

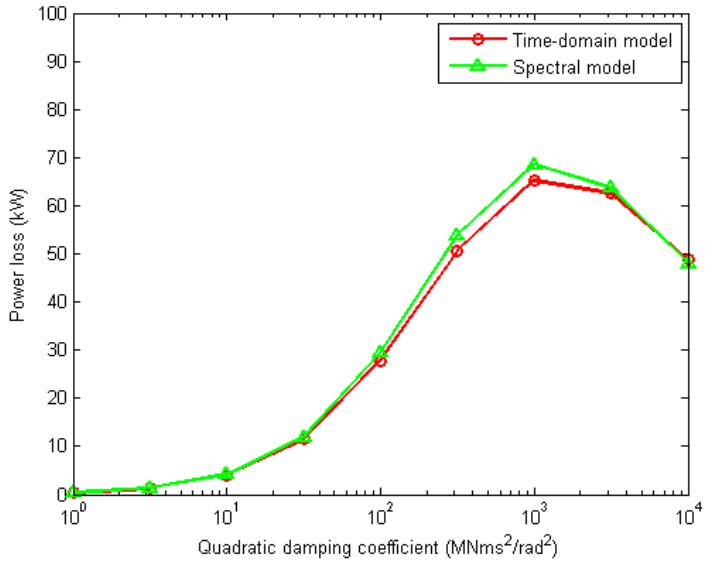

Figure 2: Comparison of estimated power loss for Oyster using time-domain and spectral-domain models.

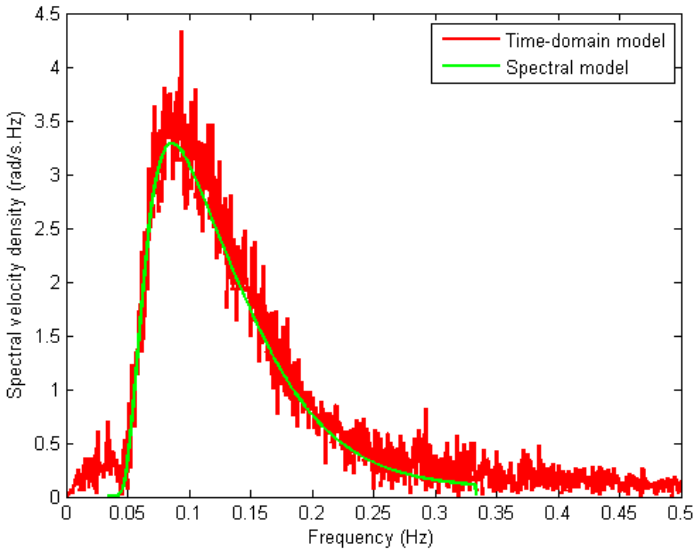

Figure 3: Comparison of the spectral velocity density for the time-domain and spectral-domain models for a quadratic damping coefficient=104 MN m s^2/rad^2.

The second comparison of spectral-domain and time-domain modelling considers wave force decoupling. Wave force decoupling occurs when a wave energy device achieves large amplitudes of motion, which result in a decrease in the incident wave force. Consequently, the performance of the device is limited in these situations. Wave force decoupling is a complex and nonlinear process, which makes it difficult to model. One approach, which will be adopted here, is to modify the incident wave torque with a factor proportional to the angle of rotation of the device. The derivation of spectral-domain model for the power starts with an expression for the force which takes this into account:

$$\boldsymbol{F = F_0 \cos A = F_0 \left(1 - \frac{A^2}{2}\right)} \qquad (2.11)$$

where $\boldsymbol{A}$ is the angle of rotation and the second order Taylor series expansion for the cosine function has been used. Substituting this force into the power expression yields:

$$\boldsymbol{P = \sum_j \langle \left(1 - \frac{A^2}{2}\right) F_0(u_1, u_2, \dots, u_j, \dots, u_n, \beta_1, \dots, \beta_n) u_j \rangle} \qquad (2.12)$$

Making the assumption that the angle of rotation and the velocity component are uncorrelated allows separation of the expected values, resulting in the following expression:

$$\boldsymbol{P = \sum_j \langle 1 - \frac{A^2}{2} \rangle \langle F_0(u_1, u_2, \dots, u_j, \dots, u_n, \beta_1, \dots, \beta_n) u_j \rangle = \langle 1 - \frac{A^2}{2} \rangle P_0} \qquad (2.13)$$

Assuming that the angle of rotation can be decomposed into sinusoidal components allows the coefficient in front of the power to be written as:

$$\langle \mathbf{1} - \frac{A^2}{2} \rangle = \mathbf{1} - \frac{\sum_j a_j^2}{4} \qquad (2.14)$$

This spectral-domain approximation is compared with the time-domain model described above. In the time-domain simulation, the wave torque is factored by the instantaneous angle of rotation at each time step. Examination of the variation of the Oyster power capture (normalized by the power capture in the absence of wave decoupling) with the root mean square of the angle of rotation shows good agreement between the time- and spectral-domain models (Figure 4).

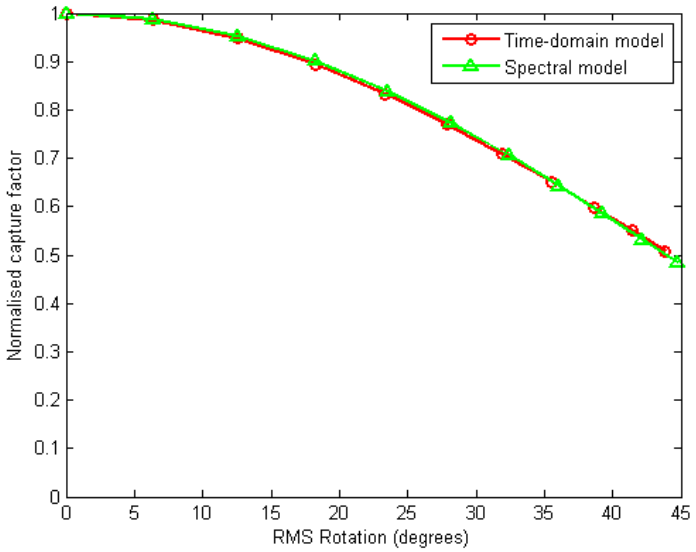

Figure 4: Comparison of effect of wave torque decoupling on power capture using time- and spectral-domain models.

Comparison of the Oyster velocity spectrums of the two model systems shows close similarity, despite the time-domain model containing more spectral noise and a small peak in the velocity density at a frequency approximately three times the peak frequency which is not captured in the spectral model (Figure 5). This is most likely a harmonic induced by the non-linear wave torque decoupling function; this harmonic could be modelled by a spectral-domain model provided that an appropriate representation of how the inter-frequency energy transfers can be produced. This second comparison of a spectral-domain representation of a wave energy converter with a time-domain model reinforces the conclusion that spectral-domain models are capable of representing nonlinear processes accurately.

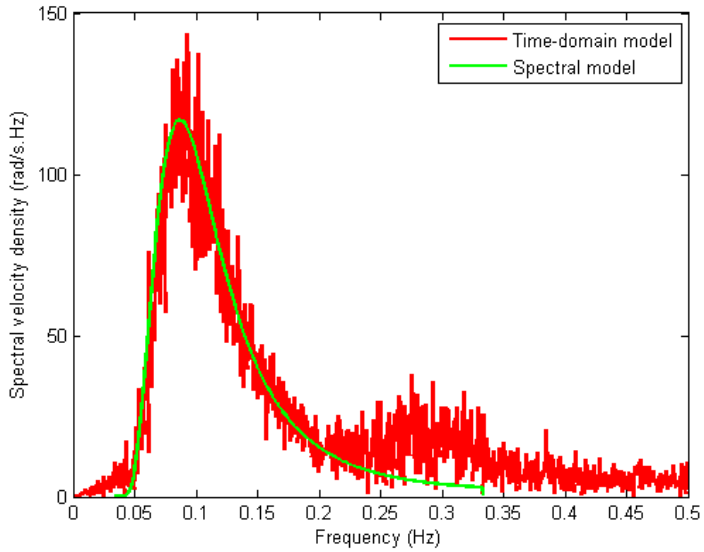

Figure 5: Comparison of the spectral velocity density for the time-and spectral-domain models for RMS Rotation=45°

2.3.2 Comparison of spectral-domain model with a wave-tank model

Further evidence to cross-validate the assertion that wave energy converters can accurately be represented by a spectral-domain model, the performance of a spectral-domain model has been compared with physical wave tank model data (Folley and Whittaker 2011). The wave energy converter modelled was an oscillating water column (OWC) device (Figure 6). The OWC modelled is a (quasi)-point absorber and thus one of the fundamental device concepts defined in WG0 D1.

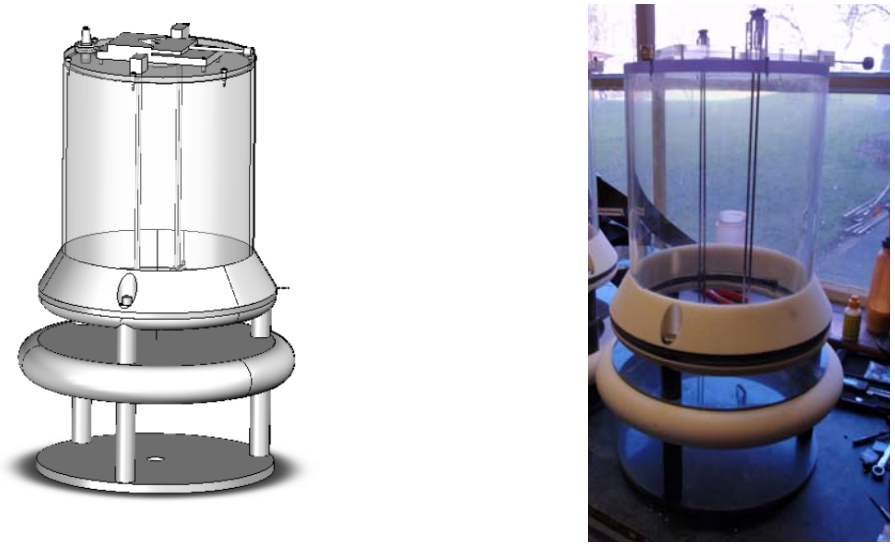

Figure 6: The Oscillating Water Column physical model

The internal diameter of the water column is 0.24 metres and it has been designed so that the water column has a natural frequency of approximately 1.0 Hz. During testing the OWC was held securely to the sea-bed in the wave-tank. Movement of the water column was measured using two twin-wire resistive wave probes positioned during testing along an axis parallel to the direction of wave propagation. The pressure in the air chamber was measured using a differential pressure transducer. This is configured with one port vented to atmosphere and the other port connected by a short flexible hose to the air chamber. A variable area orifice is used as the vent to the air chamber so that the applied damping and power extraction can be varied.

The OWC was tested in the QUB wave tank, which is 4.5 metres wide and 16 metres long. Waves are generated using a bank of six Edinburgh Designs sector-carrier wave paddles and absorbed at the other end of the wave-tank using a shoaling beach together with geo-textile matting. The beach's reflection coefficient is less than 0.1 for the full range of incident wave frequencies. During testing the OWC was located on a plateau in the wave tank floor with a local water depth of 0.4 metres.

Twelve sea-states were tested to cover a range of parameter space. Each sea-state consisted of one or more scaled Jonswap spectrum, to produce sea-states with a range of significant wave heights, energy periods and spectral shapes. The test sea-states were generated deterministically and with a pseudo-random phase[1] between each of the frequency components. The generation frequencies were chosen so that the repeat time of the wave train generated exactly equalled the data recording time of 128 seconds. This eliminates the need for windowing of the data and any problems with artificial leakage of frequency components due to the required windowing. Because the incident waves that the OWC will not be exactly the same as the waves generated at the wave paddles, surface elevation at the test location of the OWC was measured with a wave probe for each sea-state without the OWC in the tank. A sampling frequency of 64 Hz was used for the testing, which allows the frequency spectrum to be defined with a frequency step of 0.0078 Hz. However, even with deterministic wave generation this results in a significant amount of scatter in the frequency components, due the wave-tank reflections and the imperfect active absorption

[1] A psuedo-random phase means that the phase has been generated using a random number generator with a known seed and a randomisation algorithm. Thus, the phases are not genuinely random but are generated deterministically. However, the properties of the randomisation algorithm are such that they have effectively the same characteristics as genuinely random numbers.

characteristics of the wave paddles. Consequently, all measured spectra are smoothed using a symmetrical 5 point moving average.

A spectral-domain model of the oscillating water column must be derived for comparison with the physical wave tank data. The derivation of the model begins with the statement of the linear hydrodynamics of an OWC with a single degree of freedom (i.e. motion only in the heave direction):

$$\mathbf{F}(\boldsymbol{\omega}) = \left[\left\{\boldsymbol{k} - \boldsymbol{M_a}(\boldsymbol{\omega})\boldsymbol{\omega^2}\right\} + \boldsymbol{jB}(\boldsymbol{\omega})\boldsymbol{\omega}\right]\mathbf{X}(\boldsymbol{\omega}) \quad (2.15)$$

where $\boldsymbol{\omega}$ is the frequency (radians/sec), $\mathbf{F}(\boldsymbol{\omega})$ is the frequency-dependent complex wave excitation force, $\boldsymbol{k}$ is the heave stiffness of the water column, $\boldsymbol{M_a}(\boldsymbol{\omega})$ is the frequency-dependent added mass, $\boldsymbol{B}(\boldsymbol{\omega})$ is the frequency-dependent added damping, and $\mathbf{X}(\boldsymbol{\omega})$ is the frequency-dependent complex amplitude of water column heave. The hydrodynamic coefficients for the OWC were determined using the WAMIT boundary element model.

It is considered that there are two nonlinear physical mechanisms which must also be taken into account in the model: the change in air chamber pressure due to flow through the air vent, and vortex-shedding at the water column's mouth. Both of these processes can be represented using a quadratic drag term:

$$\boldsymbol{F_u}(\boldsymbol{t}) = \boldsymbol{C_D}\boldsymbol{U}(\boldsymbol{t})|\boldsymbol{U}(\boldsymbol{t})| \quad (2.16)$$

where $\boldsymbol{F_u}(\boldsymbol{t})$ is the time-dependent force due to air flow/vortex shedding, $\boldsymbol{U}(\boldsymbol{t})$ is the time-dependent velocity of water column surface, and $\boldsymbol{C_D}$ is a drag coefficient. It has been shown previously in Section 2.3.1 (Equation 2.8) that the equation can be linearised by making the drag coefficient proportional to the expected value of the water column surface velocity:

$$\mathbf{F_u}(\boldsymbol{\omega}) = \boldsymbol{2C_D}\langle|\boldsymbol{U}(\boldsymbol{t})|\rangle\mathbf{U}(\boldsymbol{\omega}) = \boldsymbol{2C_D}\sqrt{\textstyle\sum_{\boldsymbol{\omega}=\mathbf{0}}^{\infty}\frac{\boldsymbol{\omega^2}|\mathbf{X}(\boldsymbol{\omega})|^2}{\boldsymbol{\pi}}}\,\boldsymbol{\omega}\mathbf{X}(\boldsymbol{\omega}) \quad (2.17)$$

where $\mathbf{F_u}(\boldsymbol{\omega})$ is the frequency-dependent complex force due to air flow/vortex shedding, and $\mathbf{U}(\boldsymbol{\omega})$ is the frequency-dependent complex velocity of water column heave. Combining this expression with the linear hydrodynamics gives the full spectral-domain model of the OWC:

$$\mathbf{F}(\boldsymbol{\omega}) = \left[\left\{\boldsymbol{k} - \boldsymbol{M_a}(\boldsymbol{\omega})\boldsymbol{\omega^2}\right\} + \boldsymbol{j}\left\{\boldsymbol{B}(\boldsymbol{\omega}) + \boldsymbol{2}(\boldsymbol{C_{Do}} + \boldsymbol{C_{Dv}})\sqrt{\textstyle\sum_{\boldsymbol{\omega}=\mathbf{0}}^{\infty}\frac{\boldsymbol{\omega^2}|\mathbf{X}(\boldsymbol{\omega})|^2}{\boldsymbol{\pi}}}\right\}\boldsymbol{\omega}\right]\mathbf{X}(\boldsymbol{\omega}) \quad (2.18)$$

where $\boldsymbol{C_{Do}}$ is the drag coefficient of the orifice in the water column air vent and $\boldsymbol{C_{Dv}}$ is the drag coefficient of the water column mouth due to vortex shedding. Because the coefficients are only quasi-linear there is not an explicit solution to this equation; however, it can be readily solved iteratively. In the case of the OWC modelled the number of iterations required to achieve a solution was typically 4 or 5. Once the dynamics of the OWC have been solved the power capture can be

calculated as simply the sum of the power dissipation through the orifice for all the individual frequency components.

$$\boldsymbol{P_c} = \sum_{\omega=0}^{\infty} \boldsymbol{C_{Do}} \sqrt{\sum_{\omega=0}^{\infty} \frac{\omega^2 |\mathbf{X}(\omega)|^2}{\pi}} \omega^2 |\mathbf{X}(\omega)|^2 \qquad (2.19)$$

Because the drag coefficients $\boldsymbol{C_{Do}}$ and $\boldsymbol{C_{Dv}}$ are unknown, the spectral-domain model was tuned to the physical wave-tank data using these two parameters to minimize the differences in the results. This process reduces the number of statistical degrees of freedom of the comparison, and weakens the strength of the cross-validation presented here. However, with only 2 controllable parameters and 12 test sea-states the reduction in strength of validity is relatively small. Moreover, it will be seen that not only is the power capture predicted accurately, but that the spectral response of the OWC is also well predicted by the spectral-domain model.

Comparison of the power capture for the spectral-domain model and the physical model over a range of sea states shows good agreement, Figure 7.

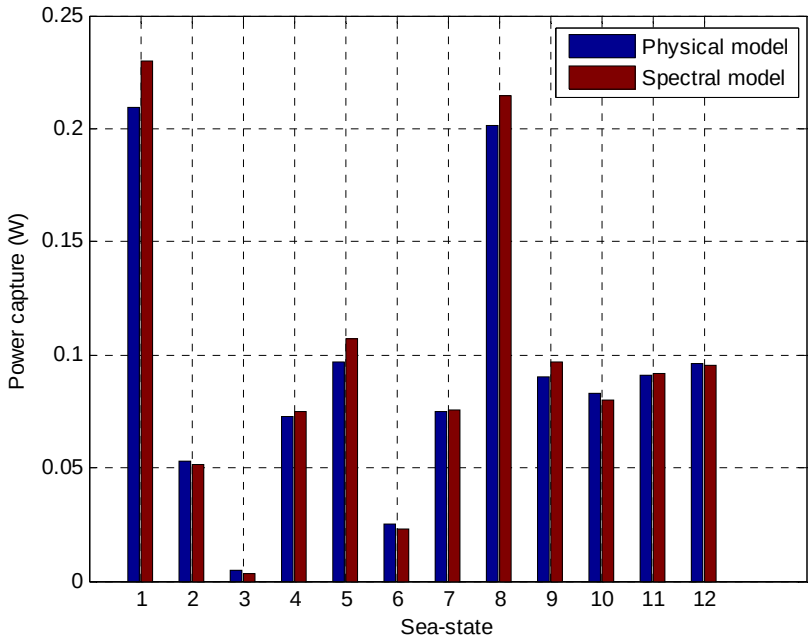

Figure 7: Comparison of spectral-domain model and physical model power captures

The average percentage error in the estimation of average power capture by the spectral-domain model error is 7%. Moreover, a large proportion of this average error is associated with sea-state 3 where the spectral-model under-estimates the power capture by 33%. However, because of the small pressures and motions in this sea-state accuracy of the instrumentation will be lower in

this case and so more prone to measurement error. Consequently, it is possible that the average error in the spectral-domain model is even lower than 7%.

Comparison of the water column heave spectral wave variance density demonstrates that the spectral-domain model is capable of capturing the spectral shape of the OWC, Figure 8.

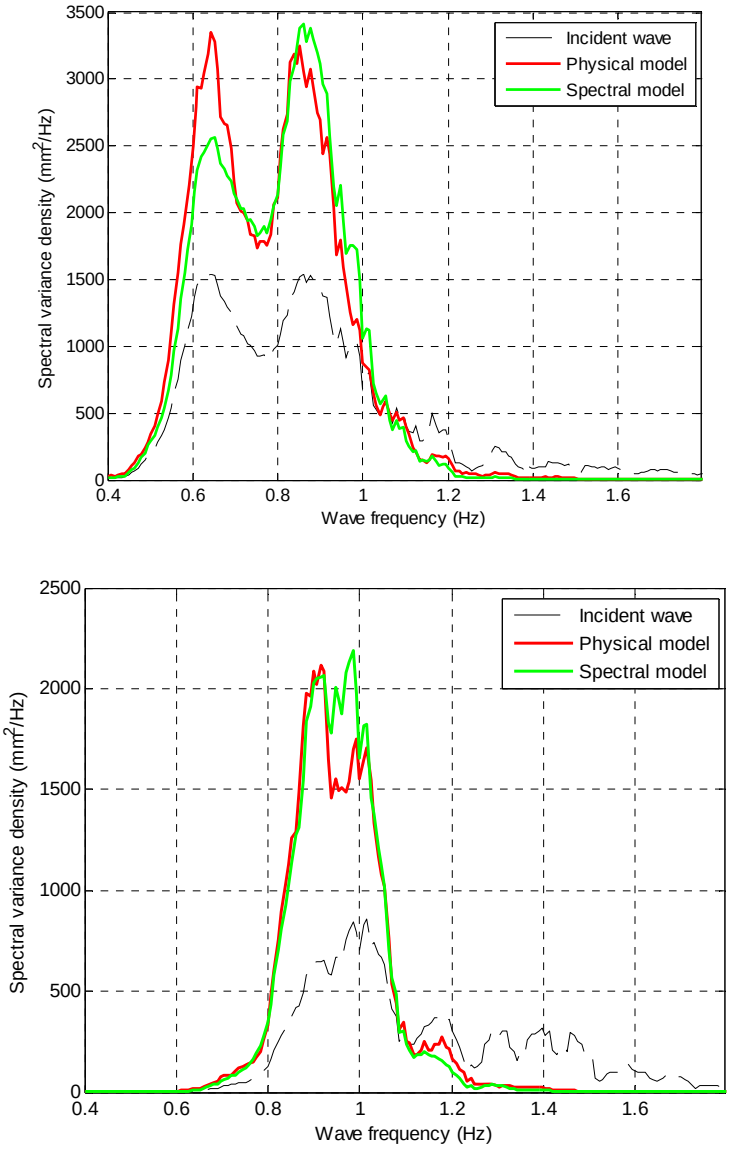

Figure 8: Comparisons of water column heave spectral variance density for the physical and spectral models for experimental sea state 1 (top panel) and sea state 9 (bottom panel).

The response amplitude operators (RAOs) for the two sea-states can be calculated by dividing the water column spectral variance density by the spectral variance density of the incident wave. It can be seen that the RAOs are also reasonably well predicted by the spectral-domain model, except

at low or high frequencies (Figure 9). It is likely that the deterioration in prediction at high and low frequencies is because the sea-state's spectral variance density in these regions is small, making predictions of the RAO less reliable due to the increased significance of noise (at high and low frequencies the motion of the water column is very small and so signal noise has a larger influence on the measured value of RAO).

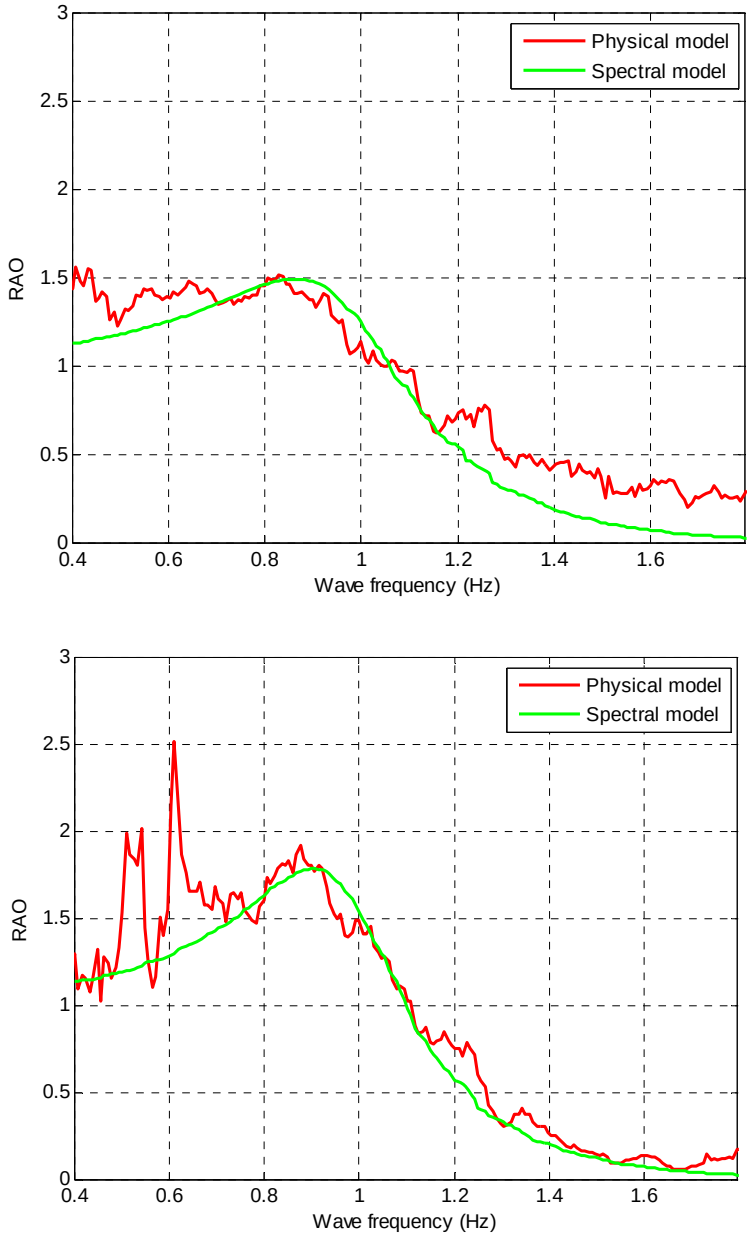

Figure 9: Comparisons of the RAOs for the physical and spectral models for sea state 1 (top panel) and sea state 9 (bottom panel)

Examination of the RAO for the twelve different sea states highlights the importance of using a quasi-linear representation for a WEC as in the spectral-domain model presented here, Figure 10. A linear representation assumes that the RAO is not dependent on sea state and is shown in Figure 10 as a red line. It can be seen that in fact the RAO is generally smaller than the linear response and varies greatly over the range of sea states. Thus it is important to include the nonlinear terms through the quasi-linear coefficient.

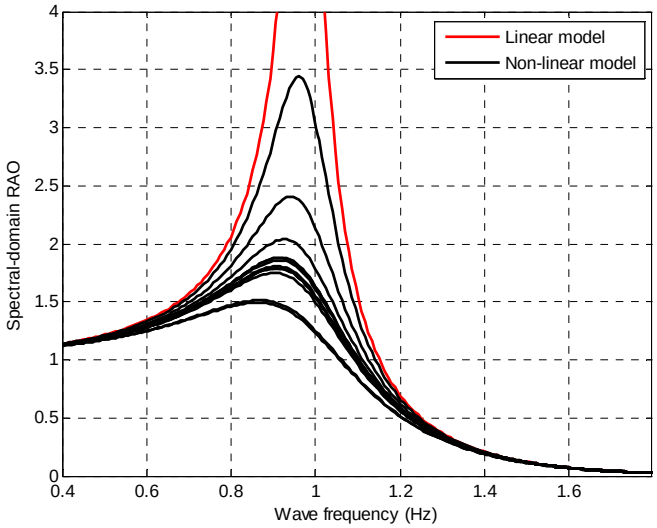

Figure 10: Variation of the RAO with the 12 sea states

The ability of spectral-domain models of wave energy converters to provide comparable results to both time-domain models as well as physical tank data is encouraging. These comparisons suggest that spectral-domain models of wave energy converters have the ability to correctly predict not only power capture for the device, but also spectral shapes and response amplitude operators as well.

3 Overview of spectral wave models

3.1 Historical development of spectral wave models

The designation "spectral wave model" refers to a numerical representation of transformation of the sea that accounts for processes such as wave propagation, wave dissipation, and wave generation. These models solve the wave action evolution equation, which is described in detail below. The main difficulty with solving this equation is the representation of the sources and sinks of energy (i.e. wave generation and dissipation processes). Although the three main categories

of source terms were identified early on as wind input, nonlinear interactions, and dissipation (due to whitecapping and bottom friction), the appropriate representation of these terms in the form of a spectral source or sink of energy was not clear. Spectral wave models went through a series of developments over the last 50 years as source term representations became more sophisticated (Komen et al., 1994). The resulting models can be classed into three different categories, as described below.

3.1.1 First generation spectral wave models

First generation spectral wave models were the simplest and earliest form of spectral wave models, solving for the energy density of the wave field as a function of frequency, direction, and one horizontal spatial dimension. First generation spectral wave models are classified as those which neglect the effects of nonlinear interactions (The SWAMP group, 1985). The dominant source of energy in these models is the wind, the influence of which is linearised. This is done by making the assumption that wind input of energy into the wave spectrum results in a linear wave growth with time. In first generation models, waves of each frequency develop independently of each other, and the spectrum gains energy from the wind until it reaches a saturation spectrum which is defined universally in the model. The main problem with first generation spectral models comes from the negligence of the nonlinear interaction terms. Because these nonlinear terms can dominate the wave energy budget in certain circumstances, the results obtained from using a first generation model can have serious errors. Examples of first generation spectral wave models include the operational forecasting model (MRI) developed at the Meteorological Research Institute of the Japanese Meteorological Agency in Tsukuba, Japan, and a regional wave statistics model (VENICE) developed at the Instituto per lo Studio della Dinamica delle Grandi Masse in Venice, Italy.

3.1.2 Second generation spectral wave models

As surface wave theory developed, it was recognized that in reality, wave frequency components do not evolve independently of each other, but are coupled through nonlinear energy transfers. Therefore, it became vital to find a representation of these nonlinear mechanisms for spectral wave models. There are two different implementations of nonlinear interactions in spectral wave models which are categorized as second generation.

The first second generation category is a coupled-hybrid model. Coupled-hybrid models are based on the fact that although the energetics of the wind-sea are dominated by the nonlinear source term, nonlinear coupling between swell components tends to be negligible. Thus, the wave spectrum can be separated into swell and wind-sea, with different physical mechanisms applied to

each portion of the wave field. Because nonlinear interactions act to force the wind-sea into a state of equilibrium, the wind-sea portion of the spectrum can be parameterized with only a few free parameters to represent the equilibrium spectral shape. The swell portion of the spectrum is represented in a discrete spectral fashion as the first-generation spectral wave models, and its evolution is dominated by the dynamical portion of the energy equation (not the source and sink terms). The advantage of this method is the ability to parameterize part of the wave field, thus reducing the computational load. However, a coupled-hybrid model does not accurately capture the evolution of the intermediate portion of the spectrum where nonlinear effects neither dominate nor are they negligible. Examples of coupled-hybrid models are the operational forecasting model of the Norwegian Meteorological Institute (NOWAMO), and the regional wave statistic model of Tohoku University in Sendai, Japan (TOHOKU).

The other category of second generation spectral wave models is known as coupled discrete models. These models do not use the separation of the wave spectrum into wind-sea and swell components. Coupled discrete models discretize the entire frequency spectrum, and solve the energy conservation equation with a nonlinear interaction source term which is highly parameterized. The full discretization of the wave spectrum means a heavier computational load, but a more accurate solution for the entire frequency range. One disadvantage of this model type is the parameterization of the nonlinear interaction term, which is not ideal. Examples of coupled discrete models are the operational forecasting model of the British Meteorological Office in Bracknell (BMO), and the regional wave statistics model developed at Scripps Institution of Oceanography in California (DNS).

3.1.3 Third generation spectral wave models

First- and second generation spectral wave models were developed independently worldwide, as can be seen from the examples listed in the previous sections. Several of the model developers joined together in an effort to use their combined experience to improve spectral wave models. The SWAMP study, carried out in the 1980s, compared several first and second generation models over a variety of model configurations (The SWAMP group, 1985). Their major conclusions were that the variability of wave spectra was not accurately captured by the parameterizations used in current spectral wave models, and that the model performance could be improved by the addition of another horizontal spatial dimension to the model configuration. Because computational resources had progressed, it was now possible to implement this next stage model, known as a third generation spectral wave model. Third generation spectral wave models contain representations of all the source terms, including a more sophisticated parameterization of nonlinear interactions, and

solve for a fully two-dimensional wave climate. Examples of third generation spectral wave models are the Simulating WAves Nearshore model (SWAN) developed at Delft University in the Netherlands, and the TELEMAC-based Operational Model Addressing Wave Action Computation (TOMAWAC) developed by EDF in Chatou, France.

3.2 Conservation of wave action

Spectral wave models are designed to represent the sea state at any given time using statistical methods, as the underlying fluid dynamics are too complicated to allow for a deterministic description of the surface wave climate. Therefore, the goal of a spectral wave model is to solve the wave action equation. Wave action, denoted by $\boldsymbol{N}$, is defined as the energy density of the direction spectrum divided by the frequency ($\boldsymbol{N = E/\sigma}$) and is a multi-dimensional variable which is a function of horizontal space, time, direction, and frequency. Wave action is conserved even in the presence of time-varying background currents, while spectral energy density is not, which is why spectral wave models solve the conservation of wave action equation given as follows:

$$\frac{\partial \boldsymbol{N}}{\partial \boldsymbol{t}} + \boldsymbol{\nabla_x} \cdot \left[\left(\overrightarrow{\boldsymbol{c_g}} + \overrightarrow{\boldsymbol{U}}\right)\boldsymbol{N}\right] + \frac{\partial \boldsymbol{c_\sigma N}}{\partial \boldsymbol{\sigma}} + \frac{\partial \boldsymbol{c_\theta N}}{\partial \boldsymbol{\theta}} = \frac{\boldsymbol{S}}{\boldsymbol{\sigma}} \qquad (3.1)$$

Here c_g is the group velocity, $\boldsymbol{U}$ is the background current, and $\boldsymbol{c_\sigma}$ and $\boldsymbol{c_\theta}$ are propagation velocities in spectral space where $\boldsymbol{\sigma}$ is the wave frequency and $\boldsymbol{\theta}$ is the wave direction. Finally, $\boldsymbol{S}$ represents any source or sink term which adds, removes or transfers energy in the system.

3.3 Convection of wave action

The first term on the left hand side of the wave action equation represents the change of wave action density in time. The next three terms are known as convection terms. In the absence of any source terms, the wave action density is conserved, and therefore these terms can only serve to move energy around in horizontal, frequency, and directional space (that is, they cannot act as sources or sinks of wave action). The first convection term represents the horizontal propagation of energy; it can be seen that the speed that the energy moves is the sum of the group velocity and the background current. The second convection term represents the shifting of energy between frequencies, which can occur because of variations in the mean currents and the water depth. Finally, the third convection term represents the shifting of energy in directional space, typically termed refraction, again due to either variable water depth or currents.

3.4 Source terms

The aggregated source term represents the mechanisms by which energy is gained and lost. Currently, in spectral wave models the aggregated source term is typically broken down into six independent components, as follows:

$$\boldsymbol{S} = \boldsymbol{S_{in}} + \boldsymbol{S_{nl3}} + \boldsymbol{S_{nl4}} + \boldsymbol{S_{wc}} + \boldsymbol{S_{db}} + \boldsymbol{S_{bf}} \quad (3.2)$$

where $\boldsymbol{S_{in}}$ represents generation of waves by the wind, $\boldsymbol{S_{nl3}}$ represents nonlinear triad interactions, $\boldsymbol{S_{nl4}}$ represents nonlinear quadruplet interactions, $\boldsymbol{S_{wc}}$ represents energy dissipation due to whitecapping, $\boldsymbol{S_{db}}$ depth-induced wave breaking, and finally $\boldsymbol{S_{bf}}$ represents bottom friction dissipation. A brief description of the source term components follows here.

Generation of waves by the wind ($\boldsymbol{S_{in}}$) occurs through two different mechanisms. Energy transfer from the wind to the waves starts with resonance with wind-induced pressure fluctuations, which leads to the growth of small waves (Phillips, 1957). This growth is linear in time. As the wave grows, it distorts the wind field, which in turn leads to faster growth of the wave. This feedback mechanism follows the resonance mechanism, and results in an exponential transfer of energy from the wind to the waves with time (Miles, 1957). The wind source term for the wave action equation takes into account both the linear and exponential growth terms. The magnitude of the source term is dependent on the wind strength and direction as well as the wave age, frequency, and direction.

Nonlinear wave-wave interactions occur when a set of waves with resonant frequencies exchange energy across the frequency spectrum. There are two types of nonlinear wave-wave interactions: triad (or three-wave) interactions ($\boldsymbol{S_{nl3}}$), which are important in shallow water, and quadruplet (or four-wave) interactions ($\boldsymbol{S_{nl4}}$), which are important at deep and intermediate water depths. Quadruplet interactions act to shift energy away from the peak spectral frequency, both to higher and lower frequencies. Triad interactions mostly tend to shift energy from lower frequencies to higher frequencies. Although it is possible to write an analytical expression for the nonlinear wave-wave interactions and solve for the wave action equation source terms, this process is computationally intensive, and therefore not commonly implemented. Instead, third generation spectral wave models use an approximation of the two interaction source terms in which the magnitude of the source term is dependent on the wave number and frequency of the existing wave action spectrum (Hasselmann et al., 1985).

Wave energy dissipation through whitecapping ($\boldsymbol{S_{wc}}$) occurs as a wave gains energy from the wind, steepens, and becomes unstable in a highly nonlinear process. Approximation of the

magnitude of this dissipation as applied in third generation spectral wave models is dependent on the wave steepness, the wave energy, and the mean frequency and wave number (Hasselmann, 1974). Wave energy dissipation also occurs due to depth-induced wave breaking ($\boldsymbol{S_{db}}$). As waves propagate towards the shoreline the shoaling water depth results in larger wave heights, which subsequently leads to instability and wave breaking. Obviously, this process is most important in shallow water. Because experimental data have shown that depth-induced breaking does not result in changes in wave spectral shape, the magnitude of the source term is simply dependent on the wave action field (Eldeberky and Battjes, 1995). The last form of energy dissipation which can act to remove energy from surface waves is bottom friction ($\boldsymbol{S_{bf}}$). Because orbital wave motions can extend down to the ocean bottom, the resulting drag must be taken into account. In third generation spectral wave models, the bottom friction source term is typically represented with a quasi-linear drag term where the drag coefficient may be determined empirically and is typically dependent on the expected value of absolute velocity at the seabed (Collins, 1972; Madsen et al., 1988).

3.5 Relationship to other wave propagation models

Ocean wave propagation models are generally sorted into two categories: phase-resolving, and phase-averaging. Phase-resolving models are time-domain models that directly solve a simplified version of the Navier-Stokes equations, which are the governing equations for fluid dynamics. There are many different forms of these wave equations. The mild slope equation model, including the parabolic and elliptic versions of it, is commonly used to estimate changes in waves in the presence of changing bottom depth or obstacles, as it captures the effects of diffraction and refraction. Mild slope equation models solve for the free surface water elevation, and as the name suggests are limited by the assumption that the bottom slope is not very steep. Boussinesq wave models are more sophisticated wave models which solve a version of the shallow water equations, thereby resolving both the free surface water elevation and the depth integrated horizontal velocities. Boussinesq wave models account for shoaling, refraction, diffraction, and frequency dispersion. The assumptions involved in deriving the Boussinesq wave model equations result in the model being most suitable for fairly long, weakly nonlinear waves.

On the other hand, spectral wave models (which clearly operate in the spectral-domain) are phase-averaging, which means that the assumption has been made that the phases of individual waves are randomly distributed. The advantage of this simplification is the ability of the phase-averaging model to solve a much larger computational domain in the same time as the smaller domain of a phase-resolving model. The disadvantage of the phase-averaging technique is the

inability to directly account for phase-dependent processes such as diffraction. However, most third generation spectral wave models have a parametric phase-decoupled model of diffraction built into the solver. This parameterization of diffraction is based on the mild-slope equation, and expresses the diffraction in terms of the directional turning rate of the individual wave components (Holthuijsen et al., 2003). This representation has been shown to produce reasonable results in most situations except for regions in close vicinity to an obstacle which blocks a large portion of the down wave view and has a high reflection coefficient. Justification for the use of a phase-averaging model for examining arrays of wave energy converter devices is presented in the next section.

3.6 Significance of phase-averaging assumption

Previous hydrodynamic numerical modelling work has shown that arrays of wave energy converters are subject to an effect known as array interaction, in which the separation distance between devices can influence the power capture of the device due to phase differences in the wave field (Thomas and Evans, 1981; Fitzgerald and Thomas, 2007). This seems to indicate that a phase-averaging model, which cannot capture these effects, is not suitable for representation of arrays of wave energy converters. However, the significant array interaction obtained in these studies was derived for monochromatic wave and idealized devices, consisting of perfectly controlled wave energy converters and clearly defined incident waves. In the real ocean, there is much uncertainty associated with the wave energy converter position, the incident waves, and the wave energy converter dynamics. In this section, statistical analysis is applied to a more realistic wave energy converter array and sea-state, and it is shown that phase-dependent array interaction effects are not as significant as previously perceived.

First, we consider the source of the uncertainties in both the incident wave field and the wave energy converter position. Incident wave fields are often represented in a simplified manner in numerical models, such as a Bretschneider spectrum which has only two parameters for input. It has been shown previously that many sea states are bimodal, a situation which is clearly poorly represented with only two parameters. Also, the method of obtaining these parameters from a scatter diagram is flawed because the binning of the data causes loss of information. However, for measured data, an incident wave field represented with a data spectrum from a buoy or other observational platform has inherent uncertainties associated with the collection and processing of that data. Alternatively, incident wave spectra which are taken from a model such as WAM have uncertainties associated with the calibration of the model.

Now consider wave energy converter position. After wave energy converters have been deployed in an array, the actual position of each device may be slightly different than the planned position, resulting in uncertainty in the device positions. Of course the array could be surveyed after the deployment, but any pre-deployment modelling will include positional uncertainty. Moreover, wave energy converters that are deployed with compliant moorings will have uncertainties in their position as they can move around in the water due to marine currents and low frequency oscillations on their moorings. Marine currents also effectively contribute to the positional uncertainty of wave energy converters, as a wave propagating with a current will travel faster between devices, effectively shortening their separation distance. Conversely, a wave propagating against a background current will travel more slowly between devices, resulting in a larger effective separation distance.

In order to evaluate the array interaction factor with the above described uncertainties taken into account, a simple statistical analysis was performed. Two examples of wave energy converter configurations were investigated. The first is of a pair of heaving truncated cylinders with a 10.0 metre diameter and 10.0 metre draft with optimum damping, and the second of a pair of surging truncated cylinders with a 10.0 metre diameter and 10.0 metre draft with optimum damping. The array interaction factors are calculated assuming that the hydrodynamics are linear, irrotational and inviscid and the hydrodynamic coefficients have been obtained using WAMIT. For both examples it is assumed that the amplitudes of motion of the WECs are unconstrained and that the wave energy converter array is aligned with the direction of propagation of waves, which should result in the largest array interaction. It can be seen that the oscillation frequency of the array interaction factors increases as the wave period decreases and the separation distance increases (Figures 11 and 12).

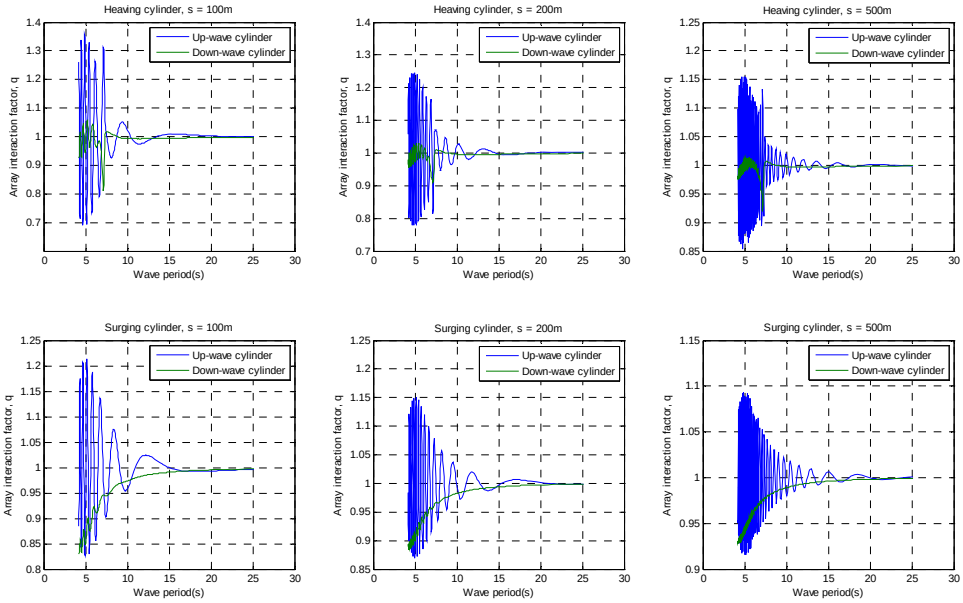

Figure 11: The variation of array interaction factors with wave period for the upwind (blue line) and downwind (green line) cylinders. The top panels are for the heaving buoy example, and the bottom panels are for the surging buoy example. The separation distance of the buoys increases from the left panels to the right panels.

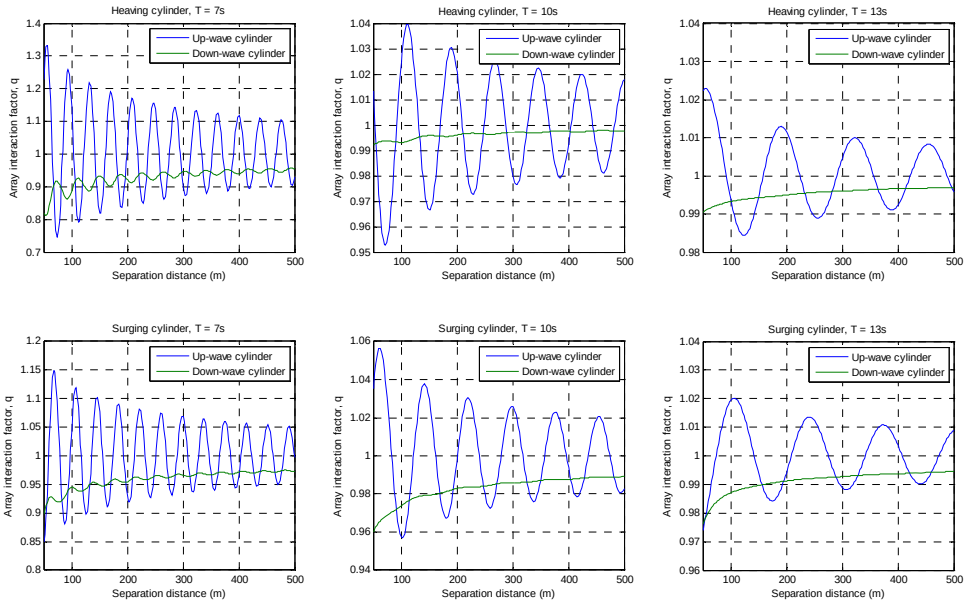

Figure 12: The variation of array interaction factors with separation distance for the upwind (blue line) and downwind (green line) cylinders. The top panels are for the heaving buoy example, and the bottom panels are for the surging buoy example. The wave period increases from the left panels to the right panels.

Next, the expected value of the array interaction factor is defined as follows:

$$\overline{\boldsymbol{q}(\boldsymbol{T},\boldsymbol{d})} = \int_0^\infty \int_0^\infty \boldsymbol{p}(\boldsymbol{T})\boldsymbol{p}(\boldsymbol{l})\boldsymbol{q}(\boldsymbol{T},\boldsymbol{l})\boldsymbol{dTdl} \qquad (3.3)$$

where $\overline{\boldsymbol{q}(\boldsymbol{T},\boldsymbol{d})}$ is the expected value of the array interaction factor $\boldsymbol{q}(\boldsymbol{T},\boldsymbol{l})$, $\boldsymbol{p}(\boldsymbol{T})$ is the uncertainty associated with the incident wave field (here approximated as uncertainty with the wave period), and $\boldsymbol{p}(\boldsymbol{l})$ is the uncertainty associated with the wave energy converter position. Assuming that the wave period and separation distance have normal distributions with standard deviations of 1.5 seconds and 10 meters respectively allows the calculation of the expected value of the array interaction factor, the variation in the expected array interaction value is much smaller than the array interaction values, and the oscillations in the array interaction factor at short wave periods and long separation distances have vanished, Figure 13. The estimate for uncertainty in the wave period is based on the uncertainty of the ERA-40 wave atlas data, which is considered typical for a wave resource analysis. The separation distance uncertainty is an estimate based on the potential drift of a WEC on its moorings and the likely magnitude of marine currents.

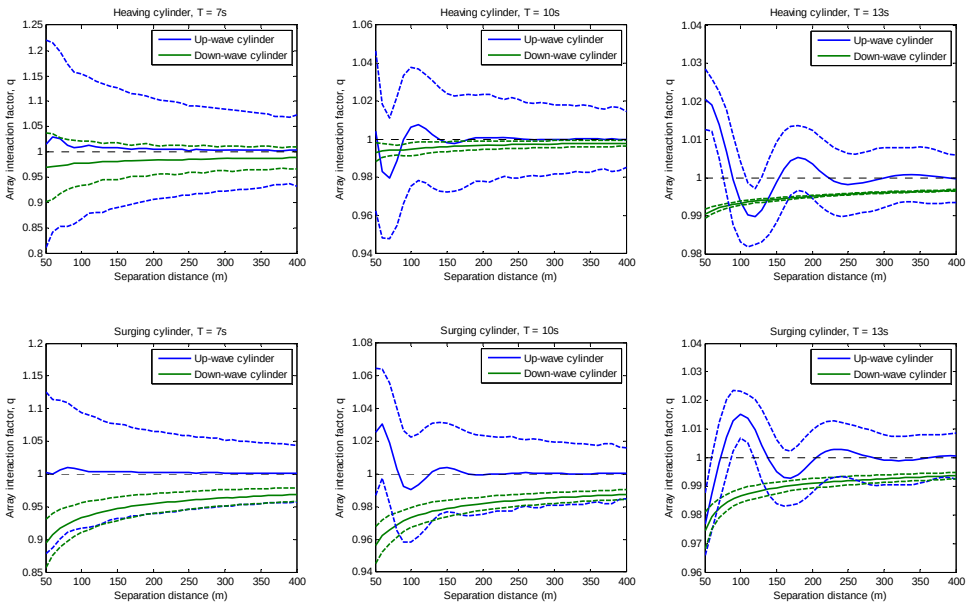

Figure 13: The variation of expected values of array interaction factor with separation distance for the upwind (blue line) and downwind (green line) cylinders. The top panels are for the heaving buoy example, and the bottom panels are for the surging buoy example. The wave period increases from the left panels to the right panels.

It is also possible to calculate the average array interaction for a sea state (as opposed to a single wave period), which is useful because it is a measure of how much the productivity of a single device in a wave farm may vary due to array interaction. The same wave energy configurations are applied now to a Bretschneider spectral shape with a directional spreading based on the cosine law: $\cos^{2s}\theta/2$, where s = 15. The magnitude of the average array interaction factor is much smaller than that for a single frequency, with oscillations of the average array interaction factor greatly reduced, and again can be seen to drop off rapidly with separation distance, Figure 14.

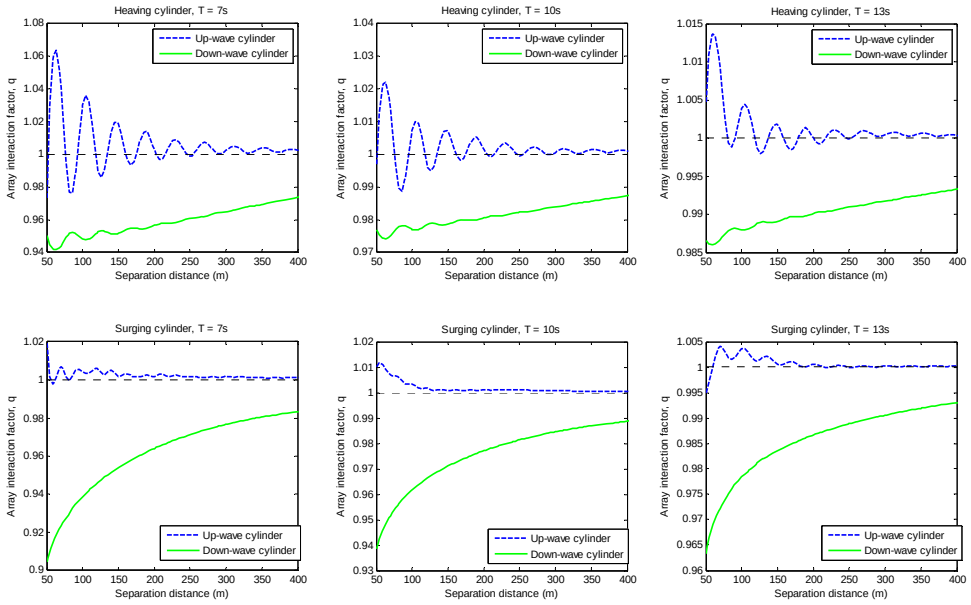

Figure 14: The variation of average array interaction factor for a sea state with separation distance for the upwind (blue line) and downwind (green line) cylinders. The top panels are for the heaving buoy example, and the bottom panels are for the surging buoy example. The wave period increases from the left panels to the right panels.

These comparisons of array interaction factors with their expected values for two simple wave energy converter configurations suggest that array effects aren't nearly as phase-dependent as initially thought; this was achieved by consideration of a more realistic scenario. It is clear that the array interaction factor is dependent on the separation distance as it can be seen to drop to zero after a certain separation distance is reached. The expected values of the array interaction factors can be seen to have smaller magnitude than the array interaction factors themselves. The results of these comparisons suggest that it will be possible to accurately capture wave energy converter array performance with a spectral wave model. If necessary, an array interaction approximation could be introduced into the wave action equation in which wave energy converters which are closer than a

set distance have an array interaction source/sink term which alters the wave action density the wave energy converter location.

4 Spatial definition of wave energy converters in a spectral wave model

4.1 Supra-grid representation of wave energy converters

Now that the use of a third generation spectral wave model to represent wave energy converter arrays has been justified, the exact nature of that representation must be derived. The first general point that must be considered is how to spatially define a wave energy converter in a spectral wave model. There is not much precedence for representing wave energy converters in spectral wave models, but the few studies that have done this have used a supra-grid representation. That is, the modelled wave farm extends across more than one grid point in the computational domain. Millar et al. (2006) used the SWAN third generation spectral wave model to look at the impact of a generic wave farm on the shoreline wave climate on the coast of Cornwall. The wave farm was represented as a four kilometre long obstacle with no distinction of individual devices. The absorption of energy by the wave farm was set to a range of percentages of the incoming wave energy (from 10 to 100%). There are several issues with using this kind of representation of wave energy converters that make it unsuitable for predictive modelling of wave farm productivity.

The representation of the wave farm as a solid block does not account for waves which pass between the devices, or array interaction effects. As such it is not possible to model the individual wave energy converters in the wave farm and therefore the effect of wave farm layout or WEC control cannot be investigated. In addition, it is also known that the response of a wave energy converter is dependent on both the frequency and direction of the incoming waves; this effect is not accounted for by the obstacle representation of a wave farm used by Millar et al.

4.2 Sub-grid representation of wave energy converters

For the PerAWaT project, it is suggested that a sub-grid representation of wave energy converters is developed, where a sub-grid representation is one in which a wave energy converter is represented at single point on the computational grid. Because the wave energy converter array model will be used to maximize energy output of wave energy device arrays, it is crucial for a realistic response of a wave energy converter to the wave field to be captured; this cannot easily be

implemented with a supra-grid representation. However, a sub-grid representation will allow the inclusion of frequency, directional, and even sea-state dependence of each individual device in the array on the background wave field. The sub-grid representation will effectively include the effects of a wave energy converter as an additional source/sink term in the wave action density equation. In addition to simply absorbing a percentage of the wave energy and transmitting the rest, the sub-grid representation may include the reflection of incident wave energy due to the presence of the wave energy converter, radiation of energy due to the motion of the wave energy converter, extraction of energy by the wave energy converter, and dissipation of energy due to turbulence around the device.

5 Formulation of wave energy converters in a spectral wave model

5.1 Overview

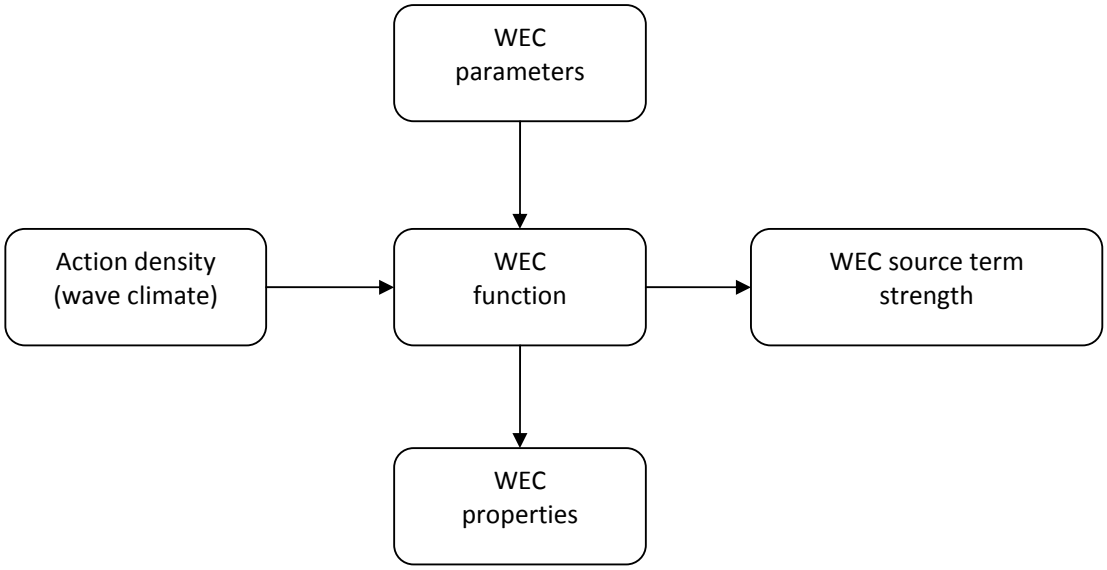

Figure 15: WEC source term component information flow

Source terms in a spectral wave model modify the action density based on the incident action density and the characteristics of the source term; the amount by which the action density is modified is typically called the source term strength. In general, the source term characteristics can be discretized into a function that defines its basic structure and parameters that control this

function. Furthermore, in addition to modifying the action density, the source term can also output its properties, which can be interrogated separately.

Figure 15 illustrates the structure and information flow in a source term suitable for representing wave energy converters (WECs). The "WEC parameters" typically include characteristics of the WEC that can be modified; for example WEC control coefficients, hydrodynamic coefficients, orientation, etc. The "WEC function" solves the system dynamics based on the WEC parameters and incident wave climate and calculates the power capture, together with the WEC source term strength. The "Action density" is defined as the wave energy density divided by the intrinsic frequency; this quantity is used because it is conserved in the presence of a background current, while energy density is not. The "WEC source term strength" is the modification made to the action density by the WEC. In general, it can be separated into three parts; reduction in the action density due to energy extracted or dissipated, increase in the action density due to wave radiation and change in the action density due to wave diffraction. Finally, the "WEC properties" can include anything calculated by the "WEC function", typically the electrical power capture is of most interest, but other properties could be provided also. The elements of the WEC source term are discussed in more detail in the following sub-sections.

5.2 WEC source term function and strength

Because of the close association of the WEC source term function and strength it is convenient to consider them together. In principle there is no restriction to the sophistication of the WEC source term function provided that it interfaces with the spectral wave model as illustrated in Figure 15. Some example structures for WEC source term functions to provide the WEC source term strength are given in Table 1.

Parameters	WEC Source term strength functions
Single parameter, p	$S(f,\theta) = p \; . \; A(f,\theta)$
Freq. dependent parameter, $p(f)$	$S(f,\theta) = p(f) \; . \; A(f,\theta)$
Non-linear parameters, $p(f)$, $p(\beta)$	$S(f,\theta) = \prod[p(f), p(\beta), A(f,\theta)]$

Table 1: Examples of possible WEC source term strength functions

Where

$S(f,\theta)$	WEC source term strength
$A(f,\theta)$	Action density
p	constant WEC parameter
$p(f)$	WEC parameter is a function of frequency

$p(\beta)$	WEC parameter is a function of another parameter, β
$\prod[..]$	A function of …

One of the simplest WEC source term functions calculates the WEC source term strength as proportional to the action density in each direction and frequency; the proportionality constant would be a single WEC parameter. The power generated could then be defined as a percentage of the WEC source term strength by a second constant parameter.

A slightly more complicated function structure would be for the WEC source term function to calculate the WEC source term strength based on a factor of proportionality that is frequency (and optionally direction) dependent. This could be obtained directly from a frequency-domain analysis. If the WEC is approximately linear then this is probably a reasonable first-order approximation to the source strength. The power generated can also be calculated directly from a frequency-domain analysis, based on a second frequency-dependent parameter.

Further levels of sophistication to the WEC source term function can be obtained by adding to the model elements that represent non-linear hydrodynamics and/or the performance of the power-take-off system, moorings, etc. These can be defined functionally or explicitly. Functional representations could be achieved by augmenting the system equations, or by using additional equations. Explicit representations can be achieved using a fixed parameter or look-up table. In general, a combination of one or more of these methods can be used to define the WEC source term function. Indeed, it is also possible to use a hybrid solution where the choice of functional representation is selected using a look-up table and any WEC source term function is acceptable provided it has the specified inputs/outputs.

Increasing the complexity and sophistication of the WEC source term function will generally increase the accuracy of both the WEC power production and the strength of the WEC source term. However, developing a very accurate function may take a significant amount of time and effort. It is expected that most of this effort will not be in specification of the WEC source term function itself, but in the development of understanding of the relevant hydrodynamics and production of a suitable system model, which is then used to specify the WEC source term function.

Although the above examples of WEC source term function and the example given in Section 5.5 the hydrodynamics are derived from a linear representation, in general this not necessary. The WEC source term function could be derived for another representation, or could be developed heuristically based on prototype performance data, wave-tank testing, numerical models or a

combination of all three. In addition, although it is attractive to consider deterministic time-domain models as being preferable or superior to statistical spectral-domain model this is not necessarily the case. The average effect of wave breaking would be very complex to solve using a time-domain models, however it can be successfully modelled using a spectral-domain model.

It is possible that particular families of WECs can be defined with similar WEC functions, which can all use the same set of parameters. This is likely to be most common for technologies in the earlier stages of development, which have not progressed sufficiently to warrant more specific representations. There is clearly a balance between the efforts of developing a flexible WEC function, suitable for a range of range of WECs and the reduced effort of bespoke WEC functions. It is likely that the balance between these two options will shift as the complexity of the WEC function develops so that generic WEC functions are most suitable in the early stages of development and bespoke function more suitable as the technology and understanding develops. It would seem sensible to decide this on a case-by-case basis, recognising that in general bespoke WEC functions may be generalised and generic WEC functions may be customised.

5.3 WEC parameters

The number and type of WEC parameters requiring specification will depend on the WEC source term function. Typically, the more accurate the function the more parameters will be needed to be specified (although in some special cases it may be possible to reduce the number of parameters required with a particularly appropriate or efficient representation of the WEC). In addition, there will generally be two types of parameters; those that will be the same for all the devices in the wave farm and those that can be different for individual devices. An example of the former type of parameter may be the diameter of the hull, whilst an example of the latter type of parameter may be the torque applied by the electrical generator. Although within the WEC source term function there is no difference between how these two types of parameters are treated, it is likely to be convenient to distinguish between them to ease the specification of the wave farm and for optimisation of the wave farm.

5.4 WEC properties

The obvious and necessary WEC property that must be output by the WEC source term function is the power generation of the WEC. By summing all of the power generated from the devices in the wave farm it is possible to calculate the wave farm power production. Integration of the wave farm power capture over all of the sea-states for a year, or over a weighted set of representative sea-states, will provide the annual wave farm energy yield. However, the output of the WEC properties is

not limited to the power generation, but can include anything that is available in the WEC source term function.

An example of an additional property that could be output by the WEC source term function is the efficiency of the secondary power conversion system. This could be used to determine whether the operating point of the secondary power conversion system is set appropriately, helping with design refinement of the wave farm. Another, more complex, example would be to output the spectral density of the WEC response or power generation, which could be used to estimate expected excursion of the WEC, or to investigate the variability of the power supply based on a spectral analysis (broad-banded spectra tend to have a more constant power production, whilst narrow-banded spectra tend to have a higher level of groupiness and so more variability in power production).

5.5 Example for a wave energy converter

A floating reaction-less heaving buoy wave energy converter (WEC) is analysed to provide an example of the type of information required to define a WEC source term in a spectral wave model. Other WECs will require different amounts and possibly types of information. Also, it is possible to define the WEC using more or less information resulting in a more or less accurate representation of the WEC's performance. The definition of the WEC used for the source term will in general depend on the stage of technological development and the extent of system knowledge that allows a suitable representation of the WEC to be produced. The information specified in this example may be typical of the extent of information available for a technology at the early stages of development.

The floating reaction-less heaving buoy consists of a compliantly-moored axi-symmetric hull below which is suspended a second body and generates power from their relative motion using a hydraulic motor and generator. The device has three operating conditions; power-generation, stand-by and survival modes. In the power generation mode the hydraulic motor is operating to provide a pressure proportional to the relative velocity, in stand-by mode the hydraulic motor is bypassed and in survival mode a valve has been closed to restrict the flow through the hydraulic motor. The actual operating condition for any particular sea-state is dependent on the incident significant wave height only.

The requirements of the WEC source term can be separated into three distinct elements. These are; analysis of the WEC hydrodynamics and dynamics; calculation of the WEC power performance and calculation of the WEC source term strength. Each of these elements will be considered separately in the following sections.

5.5.1 Analysis of the WEC hydrodynamic and dynamics

The following assumptions are made in the analysis

- Marine currents do not influence the dynamics of the WEC.
- The only motions of significance are the heave of the hull and the relative motion of the suspended body
- The moorings have a negligible effect on the dynamics of the WEC.
- In operational model the effect of the hydraulic motor can be represented as a linear damper acting on the relative motion of the hull and suspended body.
- In stand-by mode the effect of the hydraulic motor can be represented by zero damping acting on the relative motion of the hull and suspended body.
- In survival model the effect of the valve can be represented by very high linear damping acting on the relative motion of the hull and suspended body.
- The hydrodynamic coefficients (added mass, added damping, wave force and hydrostatic stiffness) are linear and can be derived using a boundary element method.
- The non-linear drag on the hull and suspended body can be represented using quadratic velocity terms.
- The device response is independent of the incident wave direction.

Although there are three different modes of operation, Equation 5.1 can be used to represent all of these conditions. The difference modes are modelled using different values of the motor damping coefficient. Equation 5.1 is a basic matrix representation of a two degree of freedom system, where the two degrees of freedom are the heave motion of the device hull and the relative motion of the suspended body. Components have been included in the model to represent quadratic drag losses due to the motion of the hull and the relative motion of the reaction body based on a quasi-linear representation as derived in Section 2.3.2. The first row of the matrix in Equation 5.1 is the dynamics of the device hull, and contains forces due to its own motion in the first column of the 2D matrix on the right-hand side and forces due to the relative motion of the suspended body in the second column.

$$\begin{bmatrix} F_h(\omega) \\ F_r(\omega) \end{bmatrix} A(\omega) = \begin{bmatrix} k_h - (M_h + I_{hh}(\omega))\omega^2 + j\omega(B_{hh}(\omega) + 2C_{Dh}U) & -I_{rh}(\omega)\omega^2 + j\omega B_{rh}(\omega) \\ -I_{hr}(\omega)\omega^2 + j\omega B_{hr}(\omega) & -\big(M_r + I_{rr}(\omega)\big)\omega^2 + j\omega(B_{rr}(\omega) + \Lambda + 2C_{Dr}U) \end{bmatrix} \begin{bmatrix} X_h(\omega) \\ R(\omega) \end{bmatrix} \quad (5.1)$$

$F(\omega)$	Hydrodynamic force coefficient
k	Hydrostatic stiffness
M	Mass

$I(\omega)$	Added mass coefficient
$B(\omega)$	Radiation damping
Λ	hydraulic motor/survival valve damping coefficient
$X_h(\omega)$	Heave motion of hull
$R(\omega)$	Relative motion of suspended body to hull
C_D	Quadratic drag coefficient
U	Expected value of absolute velocity
$A(\omega)$	Amplitude of incident wave component
h	Subscript refers to the whole device
w	Subscript refers to suspended body
wh	Subscript refers to effect of the suspended body on the hull
hw	Subscript refers to effect of the hull on suspended body

Equation 5.1 must be solved iteratively by using Equation 5.2 to calculate the expected values of absolute velocities

$$U = \sqrt{\sum_{i=1}^{n} \frac{1}{2} \omega_i^2 |X(\omega_i)|^2} \tag{5.2}$$

5.5.2 Calculation of WEC power performance

To calculate the WEC power performance the following assumptions are made

- The hydraulic motor efficiency can be defined as a function of the hydraulic power capture.
- The generator power performance can be represented by an iron loss, which is a constant power loss and a copper loss, which is proportional to the power generated.
- The maximum generator output can be imposed without changing the dynamics of the WEC

The power performance of the device can be calculated by considering the power chain as shown in Figure 16

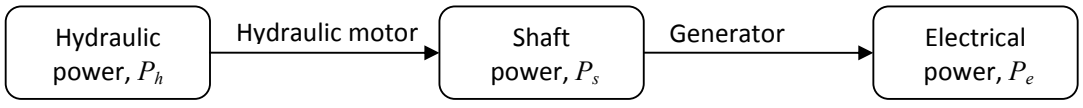

Figure 16: Power chain

The hydraulic power generated can be calculated from the hydraulic motor coefficient and the relative motion of the suspended body as given by Equation 5.3

$$P_h = \sum_{i=1}^{n} \frac{\Lambda}{2} \omega_i^2 |R(\omega_i)|^2 \tag{5.3}$$

The efficiency of a hydraulic motor is typically a function of the flow-rate and pressure. In a spectral-domain model this equates to being a function of the expected flow-rate and pressure. In this example it is assumed that the efficiency is a simple function of the hydraulic power; although a more complex efficiency function could be used with more data. Motor efficiency is typically complex and derived from experimental data. This is most easily defined using a look-up table and interpolation, although high-order polynomials or cubic splines are possible alternatives. Thus the shaft power can be simply given by Equation 5.4

$$P_s = \eta(P_h) P_h \tag{5.4}$$

Where

$\eta(P_h)$ hydraulic motor efficiency is a function of the hydraulic power

Finally, the electrical power can be obtained from the shaft power using Equation 5.5

$$P_e = \eta_{copper} P_s - P_{iron} \tag{5.5}$$

Where

η_{copper} copper loss efficiency coefficient

P_{iron} iron loss power coefficient

Finally, if the electrical power generation is greater than the electrical plant rating then the power is limited to the plant rating.

Clearly this power chain calculation is only required when the device is in operational mode, in stand-by and survival modes the power capture can be assumed to be zero.

5.5.3 Calculation of the WEC source term strength

The WEC source term strength is constructed from the effects of the radiated and diffracted waves together with the extraction of energy through the hydraulic motor and drag losses. The hydrodynamic model assumes that there are no non-linear transfers of energy between frequencies and so there must be an energy balance at each frequency. The hydrodynamic model also assumes

that wave radiation and diffraction are linear, i.e. they are proportional to the amplitudes of motion and incident wave component respectively. However, because phase is important the net radiated/diffracted wave amplitude must be used to determine the energy in the radiated/diffracted wave. Equation 5.6 shows the calculation of this generated wave amplitude

$$\xi_{\varphi}(\omega,\theta) = \alpha_h(\omega)X_h(\omega,\varphi) + \alpha_R(\omega)R(\omega,\varphi) + \beta(\omega,\theta-\varphi)A(\omega,\varphi) \quad (5.6)$$

Where

$\xi_{\varphi}(\omega,\theta)$ Generated wave amplitude at frequency, ω, and in direction, θ, due to a wave from direction, φ

φ Direction of incident wave propagation

$\alpha(\omega)$ Radiated wave coefficient

$\beta(\omega,\theta)$ Diffracted wave coefficient

The energy balance equation is then most easily calculated using the generated wave amplitude so that the reduction in wave energy flux of the incident wave component is equal to the sum of the energy sinks (radiated/diffracted wave, power extracted, power lost) as given by Equation 5.7

$$\Delta E_f(\omega,\varphi) = \sum_{i=1}^{n} \tfrac{1}{2}\rho g\left|\xi_{\varphi}(\omega,\theta_i)\right|^2 C_g(\omega) + \tfrac{1}{2}(\Lambda + 2C_{Dw}U)\omega^2|R(\omega,\varphi)|^2 + \tfrac{1}{2}2C_{Dh}U\omega^2|X_h(\omega,\varphi)|^2 \quad (5.7)$$

Where

$\Delta E_f(\omega,\varphi)$ Change in wave energy flux in the direction of wave propagation, φ

$C_g(\omega)$ Group velocity of radiated/diffracted wave

In addition, because the hydrodynamics are assumed to be linear then the energy balance can be calculated independently for each directional component and then the net effect calculated by simple linear summation of the directional components as given by Equation 5.8.

$$S_{wec}(\omega,\theta) = \sum_{i=1}^{n} \tfrac{1}{2}\rho g\left|\xi_{\varphi_i}(\omega,\theta)\right|^2 C_g(\omega) - \Delta E_f(\omega,\theta) \quad (5.8)$$

Where

$S_{wec}(\omega,\theta)$ Source strength at frequency, ω, and in direction, θ

$\xi_{\varphi_i}(\omega,\theta)$ Generated wave amplitude at frequency, ω, and direction, θ, due to incident wave from direction, φ_i

5.5.4 Summary of WEC source term specification

The WEC source term can be considered as consisting of two components; the software code and the design data. The software code must implement the 8 equations above and the design data must supply the required parameters. The two tables below summarise the source term specification requirements

Software code
Define mode of operation
Compare significant wave height to operational thresholds
Solution of non-linear WEC hydrodynamics and dynamics
Solve quasi-linear system
Calculate expected amplitudes of motion
Iterate quasi-linear system
Calculation of power train performance
Calculate hydraulic power
Calculate hydraulic motor efficiency -> Shaft power
Calculate generator efficiency -> Electrical power
Calculation of WEC source strength
Calculate net amplitude of radiated/diffracted wave
Calculate reduction in energy flux for wave components
Calculate WEC source strength

Table 1: Specification of software code

Parameter	Symbol	Dimensions
Significant wave height thresholds	-	[2 × 1]
Wave force coefficient	F	[2 × n]
Added inertia	I	[4 × n]
Added damping	B	[4 × n]
Heave stiffness	k	[2 × 1]
Mass	M	[2 × 1]
Drag coefficient	C_D	[2 × 1]
Hydraulic motor coefficient (operational)	Λ	[1 × 1]
Hydraulic motor coefficient (survival)	Λ	[1 × 1]
Hydraulic motor efficiency	η	[1 × p]
Copper loss coefficient	η_{copper}	[1 × 1]
Iron loss coefficient	P_{iron}	[1 × 1]
Electrical plant rating	-	[1 × 1]
Radiated wave coefficient	α	[2 × n]

Parameter	Symbol	Dimensions
Diffracted wave coefficient	β	[m × n]
Number of wave directional components	m	1
Number of wave frequency components	n	1
Number of power levels at which efficiency is defined	p	1

Table 2: Design data

5.6 Discussion of WEC source term specification

It can be seen that even with the simplifying assumptions made the amount of data required to define the WEC source term is relatively large. On implementation it may be found that some assumptions can be removed without significantly increasing the complexity of the software code or design data requirements. However, it is likely that in many cases the assumptions will be associated with the limited understanding of the WEC performance or operation. An example of this is the hydraulic motor coefficient, which approximately proportional to the flow-rate through the motor. In this device it has been assumed that the rotational speed of the motor is constant, but in general this will not be the case. Improved power capture may be achieved by a variable speed motor, but understanding the relationship between the rotational speed and the maximum electrical power generation requires an effort that may not have been undertaken. Thus, in this case the assumption is made not only to simplify the model, but because an appropriate control strategy is not known and a constant speed motor is a reasonable first-order approximation.

It is also possible that additional assumptions can be made that do not significantly reduce the accuracy of the model, but simplify the implementation. A candidate for this additional simplification is the inclusion of the diffracted wave. For a small device the diffracted wave will typically be much smaller than the radiated wave and it may be possible to ignore it without a significant reduction in the accuracy of the wave farm power production estimate. The diffracted wave coefficient is particularly significant in the design data specification because it is an [n × n] data-set and may contain more data than all the rest of the design data. Moreover, the calculations associated with the diffracted wave are also relatively computationally demanding and it may be that the extra effort is not justified based on its limited effect on estimated power production. Clearly, as with all assumptions, their significance should be assessed on an individual case basis.

This example describes the production of a spectral-domain representation of a point absorber WEC, which could be used in a spectral wave model for modelling a wave farm. Depending on the method used to develop the representation the equations defining the WEC source term strength the function could look very different, as could the WEC parameters, for other WECs. However, in

general, the representations of other types of wave energy converters, including the fundamental device concepts, can be developed using the same framework and can be represented in a spectral wave model. This means that it is a universally applicable representation of WECs for modelling wave farm productivity.

6 References and bibliography

Babarit A., Borgarino B., Ferrant P. and Clément A. [2009] Assessment of the influence of the distance between two wave energy converters on the energy production. In: Proceedings of 8th European Wave and Tidal Energy Conference, Uppsala, Sweden

Backer G. D., Vantorre M., Beels C., Rouck J. D. and Frigaard P. [2009] Performance of closely spaced point absorbers with constrained floater motion. In: Proceedings of 8th European Wave and Tidal Energy Conference, Uppsala, Sweden

Beels C., Troch P., De Visch K., De Backer G., De Rouck J. and Kofoed J. [2009] Numerical simulation of wave effects in the lee of a farm of Wave Dragon wave energy converters. In: Proceedings of 8th European Wave and Tidal Energy Conference, Uppsala, Sweden

Bellew S., Stallard T. and Stansby P. K. [2009] Optimisation of a Heterogeneous Array of Heaving Bodies. In: Proceedings of 8th European Wave and Tidal Energy Conference, Uppsala, Sweden

Booij, N., Holthuijsen, L.H. and R.C. Ris, [1996] The SWAN wave model for shallow water, Proc. 25th Int. Conf. Coastal Engineering., Orlando, USA, Vol. 1, pp. 668-676.

Child B. and Venugopal V. [2007] Interaction of waves with an array of floating wave energy devices. In: Proceedings of 7th European Wave and Tidal Energy Conference, Porto, Portugal

Collins, J.I. [1972] Prediction of shallow water spectra, J. Geophys. Res., 77, No. 15, pp.2693-2707

Cruz J., Sykes R., Siddorn P. and Eatock Taylor R. [2009] Wave Farm Design: Preliminary Studies on the influences of Wave Climate, Array Layout and Farm Control, In: Proceedings of 8th European Wave and Tidal Energy Conference, Uppsala, Sweden

Delauré, Y.M.C. and Lewis, A., [2003] 3D hydrodynamic modelling of fixed oscillating water column wave power plants by a boundary element methods, Ocean Engineering, 30: 309-330.

Demirbilek Z. and Vincent L. [2002] Water waves mechanics. In: Coastal Engineering Manual, Part II, Hydrodynamics, Chapter II-1, Washington, DC

DHI, [2008] Mike21 Spectral Wave Module - Scientific documentation, DHI.

Eldeberky, Y. and J.A. Battjes. [1996]: Spectral modelling of wave breaking: Application to Boussinesq equations, J. Geophys. Res., 101, No. C1, pp. 1253-1264

Evans D. V. [1979] SOME THEORETICAL ASPECTS OF THREE-DIMENSIONAL WAVE-ENERGY ABSORBERS. In: Proceedings of 1st Symposium on Ocean Wave Energy Utilization, Gothenburg

Evans, D.V., [1980] Some Analytic Results for Two and Three Dimensional Wave-energy Absorbers. In: B. Count (Editor), Power from Sea Waves, Edinburgh, UK, pp. 213-249.

Evans D. V. [1981] Maximum wave-power absorption under motion constraints. Applied Ocean Research 1981; 3(4):200-203

Evans, D.V., [1981] Power from Water Waves. Ann. Rev. Fluid Mech., 13: 157-87.

Evans, D.V., [1985] The Hydrodynamic Efficiency of Wave-Energy Devices. In: D.V. Evans, D.V. and A.F.d.O. Falcao (Editors), Hydrodynamics of Ocean Wave-Energy Utilisation. Springer-Verlag, Lisbon, pp. 1-34.

Falcao, A.F. de and Rodrigues. R.J.A., [2002] Stochastic modelling of OWC wave power plant performance, Applied Ocean Research, 24: 59-71.

Falnes, J., [1980] Radiation impedance matrix and optimum power absorption for interacting oscillators in surface waves. Applied Ocean Research, 2(2): 75-80.

Falnes, J., [2002] Ocean Waves and Oscillating Systems. Cambridge University Press.

Fitzgerald C. and Thomas G.[2007] A preliminary study on the optimal formation of an array of wave power devices. In: Proceedings of 7th European Wave and Tidal Energy Conference, Porto, Portugal

Fitzgerald C. [2007] Optimal configurations of arrays of wave-power devices. MSc Thesis. University College Cork

Folley, M. and Whittaker, T. [2009]. The effect of sub-optimal control and the spectral wave climate on the performance of wave energy converter arrays, Applied Ocean Research 31:260-266

Folley, M. [2010] Issues with physical modelling wave energy converter arrays, Internal report QUB MF 101112-01a

Folley, M and T. Whittaker, [2010]. “Spectral modelling of wave energy converters”, *Coastal Engineering*, Vol. 57, pp 892-897.

Folley M. and Whittaker T [2011] Validating a spectral-domain model of an OWC using physical model data, *Abstract submitted to 9th* European Wave and Tidal Energy Conference, Southampton, UK

Hasselmann, K. and Collins, J.I., [1968] Spectral dissipation of finite-depth gravity waves due to turbulent bottom friction. Journal of Marine Research, 26(1): 1-12.

Hasselman, K [1974]. “On the spectral dissipation of ocean waves due to white capping”, *Boundary Layer Meteorology*, Vol. 6, pp 107-127.

Hasselmann, S., K. Hasselmann, J.H. Allender and T.P. Barnett, 1985: Computations and parameterizations of the nonlinear energy transfer in a gravity wave spectrum. Part II: Parameterizations of the nonlinear transfer for application in wave models, J. Phys. Oceanogr., Vol. 15,pp. 1378-1391

Holthuijsen, L.H., Herman, A. and Booij, N. [2003] Phase-decoupled refraction/diffraction for spectral wave models, Coastal Engineering, Vol. 49, pp. 291-305

Holthuijsen, L.H., [2007] Waves in Oceanic and Coastal Waters. Cambridge University Press, Cambridge.

Justino P. and Clement A. [2003] Hydrodynamic performance for small arrays of submerged spheres. In: Proceedings of 5th European Wave Energy Conference, Cork, Ireland, 2003. p. 266 - 273

Komen, G.J. et al., [1994] Dynamics and Modelling of Ocean Waves. Cambridge Univ. Press, Cambridge, UK.

McCabe, A.P., Aggidis, G.A. and Stallard, T.J., [2006] A time-varying parameter model of a body oscillating in pitch. Applied Ocean Research, 28(6): 359-370.

McCabe, A.P., Bradshaw, A. and Widden, M.B., [2005] A time-domain model of a floating body using transforms, 6th European Wave and Tidal Energy Conference, Glasgow, UK, pp. 281-288.

McIver P. [1994] Some hydrodynamic aspects of arrays of wave-energy devices. Applied Ocean Research 16(2):61-69

Madsen, O.S., Y.-K. Poon and H.C. Graber [1988] Spectral wave attenuation by bottom friction: Theory, Proc. 21th Int. Conf. Coastal Engineering, ASCE, 492-504

Mavrakos S. A. and McIver P. [1997] Comparison of methods for computing hydrodynamic characteristics of arrays of wave power devices. Applied Ocean Research 19(5-6):283-291

Mei, C.C. and Newman, J.N., [1980] Wave power extraction by floating bodies, 1st Symposium on Wave Energy Utilisation, Gothenburg, Sweden

Michel W. H. [1999] Sea spectra revisited. Marine Technology 36(4):211-227

Miles, J.W. [1957] On the generation of surface waves by shear flows. J. Fluid Mech., Vol. 3, pp. 185 –204

Millar, D.L., H.C.M. Smith, and D.E. Reeve, [2006] Modelling analysis of the sensitivity of shoreline change to a wave farm, Ocean Engineering, Vol. 34, pp.884-901.

Newman, J.N., [1977] Marine Hydrodynamics. MIT Press, Cambridge, Massachusetts, USA

Phillips, O.M., [1957] On the generation of waves by turbulent wind. J. Fluid Mech., Vol. 2, pp. 417– 445

Simon M. J. [1982] Multiples scattering in arrays of axisymmetric wave-energy devices - A matrix method using a plane-wave approximation. Journal of Fluid Mechanics 120:1-25

SWAMP Group: J.H. Allender, T.P. Barnett, L. Bertotti, J. Bruinsma, V.J. Cardone, L. Cavaleri, J. Ephraums, B. Golding, A. Greenwood, J. Guddal, H. Günther, K. Hasselmann, S. Hasselmann, P. Joseph, S. Kawai, G.J. Komen, L. Lawson, H. Linne, R.B. Long, M. Lybanon, E. Maeland, W. Rosenthal, Y. Toba, T. Uji and W.J.P. de Voogt, [1985] “Sea Wave Modelling Project (SWAMP), An inter-comparison study of wind wave prediction models, Part 1: Principal results and conclusions, in Ocean Wave Modelling”. Plenum Press, 256p.

Thomas G. and Evans D. V. [1981] Arrays of three-dimensional wave-energy absorbers. Journal of Fluid Mechanics 108:67-88

Thomas S., Weller S. and Stallard T. J. [2008] Float response within an array: Numerical and experimental comparison. In: Proceedings of Second International Conference on Ocean Energy, Brest, France

Tucker, M.J. and Pitt, E.G., [2001] Waves in Ocean Engineering, Elsevier, Oxford, UK

Venugopal V. and Smith G., [2009] Wave climate investigation for an array of wave power devices, In: 7th European Wave and Tidal Energy Conference, Aporto, Portugal.

WAMDI Group, [1988] The WAM model - a third generation ocean wave prediction model. Journal of Physical Oceanography, 18: 1775-1810.

Whittaker, T. and Folley, M., [2007] The Oyster wave energy converter, In: 7th European Wave and Tidal Energy Conference, Aporto, Portugal.